Role of EXO1 and 53BP1 in DNA damage signalling

der Naturwissenschaftlichen Fakultät der

Gottfried Wilhelm Leibniz Universität Hannover

zur Erlangung des Grades

DOKTOR DER NATURWISSENSCHAFTEN

Dr. rer. nat.

genehmigte Dissertation

von

M.Sc. Kodandaramireddy Nalapareddy

Geboren am 05.11.1977 in Lingalapuram Village, Indien.

HANNOVER 2007

Referent: Prof. Dr. K.L. Rudolph

Koreferentin: Prof. Dr. R. Hass

Tag der Promotion: 30. November 2007

The following study has been carried out under the supervision of Prof. Dr. K. L. Rudolph, Department of Gastroenterology, Hepatology and Endocrinology, Hannover Medical School, Hannover, Germany between June 2004 and August 2007.

Declaration: Here with I declare that the study has been done by my own under the guidance of Prof. Dr. K. L. Rudolph and all the information provided is novel and true and has not been submitted to any other institute or University to obtain any other degree.

Kodandaramireddy Nalapareddy

Referee   :   **Old address:**
                        Prof. Dr. K. L. Rudolph,
                        Department of Gastroenterology, Hepatology and Endocrinology,
                        Hannover Medical School,
                        Hannover, Germany

                        Present Address:
                        Prof. Dr. K. L. Rudolph, Director,
                        Institut für molekulare Medizin und Max-planck Forschergurppe für
                        stemmzellalterung, Albert-einstein-Allee 11, 89081 Ulm.

Co-referee   :   Prof. Dr.rer.nat. Ralf Hass, AG Biochemie und Tumorbiologie.
                        Klinik für Frauenheilkunde und Geburtshilfe
                        Medizinische Hochschule Hannover
                        Carl-Neuberg-Str. 1,30625 Hannover

Co-referee   :   Prof. Dr.Hans-Jörg Jacobsen,
                        Institute of Genetics, Plant Biotechnology Section,
                        Herrenhaeuser Str-2, D-30419, Hannover.

Acknowledgements

I am very grateful to my supervisor Prof. Dr. K. L. Rudolph for giving me the opportunity , encouragement and support through out my doctorial work to pursue my research and also I am grateful to Prof. Dr. M. P. Manns for giving me opportunity to pursue my research in Hannover Medical School. I would like to thank Prof. Dr. R. Hass, Department of Biochemistry and Tumorbiology, Hannover Medical School, Hannover for the help to pursue my doctorial thesis.

I would like to thank the colleagues from Nuclear Medicine, Hannover Medical School for their help to Irradiate mice and cells which were necessary for my doctorial thesis work

I would like to thank my colleagues Andre´, Andrea, Aaheli, Arpita, Annika, Elvira, Holger, Harshvardan, Hong, Luis, Parisa, Satyanarayana, Sonja, Ujala, Yvonne, Zhenyu for valuable discussions and co-operation through out my research work.

I would like to thank my wife N.Padmavathi devi for valuable discussions and co-operation through out my research work.

.

Contents

Zusammenfassung

Disfunktionelle Telomere induzieren eine DNA Schädigungsantwort in Folge auf Aktivierung von DNA Schädigungs-Signalkontrollpunkten, wodurch Zellzyklusarrest oder Apoptose ausgelöst wird. Für die Kontrollpunktsaktivierung in der Bäckerhefe wird ein Exonuklease 1 (EXO1) abhängiges Prozessieren von disfunktionellen Telomeren und die Generierung von einzelsträngiger DNA (ssDNA) benötigt. Es ist unbekannt, ob auch in Säugerzellen EXO1 eine Rolle in der Induktion von Kontrollpunkten in Antwort auf Telomerdisfunktion oder DNA Doppelstrangbrüchen spielt. Unsere Studien haben gezeigt, dass eine Deletion der Nuklease-Domäne von Exo1 die DNA Schädigungsantwort sowohl im Darmepithel von Mäusen als auch in Mausohr-Fibroblasten in Antwort auf Telomerdisfunktion auf γ-Bestrahlung verhindert. Die verminderte Formierung von DNA Schädigungs-Foci korrelierte mit einer reduzierten Induktion von Proteinen wie ATR, p53, CHK2 und p21, die in der DNA Schädigungssignalkaskade Exo1 nachgeschaltet sind. Die Deletierung von Exo1 zeigt keinen lebendsverlängernden Effekt bei Rad50 Knockin Mäusen, die eine hypermorphe Mutation des Rad50 Gens exprimieren. Allerdings zeigte sich, dass die Deletion von 53BP1 zu einer höheren Überlebensrate von hypermorphen Rad50 Knockin Mäusen führt. Diese Studien zeigen erstmals, dass Exo1 sehr weit oben in der DNA Schädigungskaskade eine DNA Schädigungsantwort in Antwort auf Telomerdysfunktion und γ-Bestrahlung in Säugerzellen induziert. Des weiteren liegt 53BP1 *in vivo* in der DNA Schädigungssignalkaskade unterhalb von Rad50 .

Schlagwörter: Zellzyklus, DNA Schädigung, Telomere Verkürzung

Abstract

Dysfunctional telomeres induce a DNA damage response leading to cell cycle arrest or apoptosis due to activation of DNA damage signalling pathway. In budding yeast, Exonuclease-1 (Exo1) dependent processing of dysfunctional telomeres and generation of single stranded DNA (ssDNA) is required for checkpoint induction. It is unknown whether Exo1 has a role for checkpoint induction in response to telomere dysfunction or DNA breakage in mammalian cells. Our study shows that deletion of the nuclease domain of Exo1 impaired the DNA damage signalling in mouse intestinal epithelium in response to telomere dysfunction and γ-irradiation (IR) and also in mouse ear fibroblasts in response to IR. Impaired DNA damage foci formation correlated with diminished induction of downstream DNA damage signals including ATR, p53, CHK2 and p21. Exo1 deletion did not rescue survival of knockin mice carrying a hypermorphic Rad50 mutation. But deletion of 53BP1, a DNA damage signalling protein rescued the survival of mice with hypermorphic Rad50 mutation. This study provides the first evidence that Exo1 initiates the very upstream induction of DNA damage signals in mammalian cells in response to telomere dysfunction and Irradiation and 53BP1 is a down stream target of Rad50 in vivo in the DNA damage signalling pathway.

Key words: Cell Cycle, DNA damage, Telomere shortening.

1. Introduction

1.1. The end replication problem of eukaryotic cells

In a cell, the nucleus is one of the most important organelle whose function is to maintain the integrity of the genes and to control the activities of the cell. The nucleus harbours chromosomes which are made up of nucleic acid known as DNA. During each round of cell division the DNA has to be divided for which it has to be replicated first. DNA polymerase is the enzyme which performs the replication of DNA. DNA polymerase synthesizes a new strand of DNA as it moves along the template strand in the 3' to 5' direction. This occurs on the 3' to 5' strand (leading strand) of a chromosome. The DNA polymerase moves un-interruptedly from an origin of replication until it meets another bubble of replication or the end of the chromosome. In contrast the replication of the lagging strand (5' to 3' strand) is discontinuous and the DNA polymerase requires small RNA-primers for the initiation of DNA-replication. When the replication fork opens, the DNA polymerase binds to the RNA-primer and begins to synthesize a section of the complementary strand - called an `Okazaki fragment´ proceeding in the opposite direction of the movement of the replication fork. This continues until very close to the end of the chromosome. After the synthesis of okazaki fragments, the DNA ligase ligates the okazaki fragments together. After the synthesis of DNA from the RNA primer at the end of the chromosome will be digested and the stretch of the site where RNA was digested will remain unduplicated which is known 'as the end replication problem'.
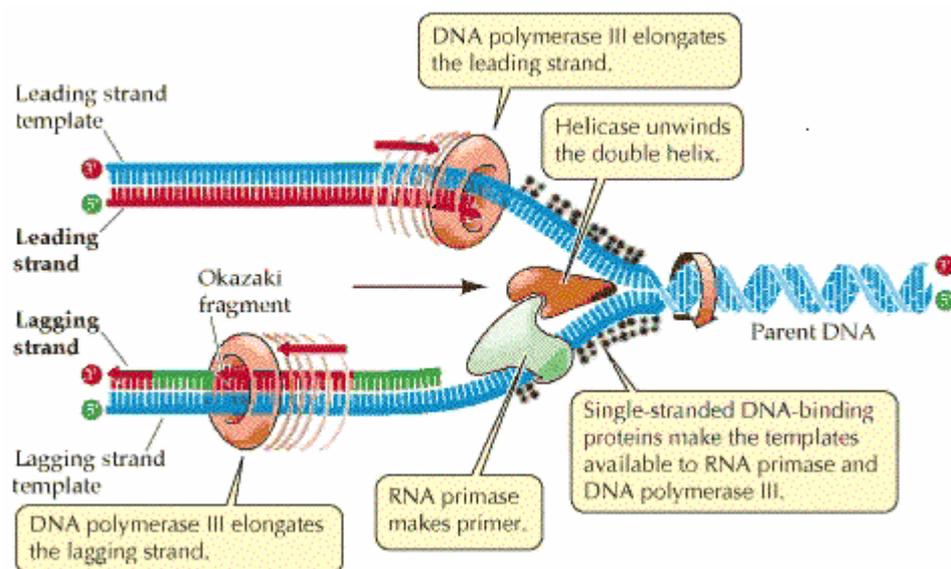
Fig.1.The end replication problem. The figure shows the replication fork where the DNA polymerase is involved in both continuous leading strand synthesis and discontinuous lagging strand synthesis by preparing

okazaki fragments. (The cell cycle: DNA replication, mitosis and cancer, Chapter 17, *Addison wisely Longman*) (Fig source www.contexo.info/DNA_Basics/DNA%20Replication.htm).

1.2. Telomeres - structure and function

Telomeres are tandem repeats of the sequence (TTAGGG)n which are present at the ends of chromosomes containing a 3` G-rich over hang at the end of the chromosome. The lengths of the telomeres are approximately about 10-15 kilobases (Kb) in humans and 40-60 Kb in inbred mouse strains (Aviv et al., 2003; Hemann and Greider, 2000; Liu et al., 2002; Greider and Blackburn, 1989). Telomeres are protected by several telomere binding proteins such as Trf1,TIN2, POT1, Trf2, Tankyrase etc which helps the telomeres to form a t-loop like structure which helps to hide the free ends of telomeres in this loop and prevents the free ends of telomeres from being recognised as DNA damage.(de Lange, 2005).

Fig.1.2.1. Telomere structure in open form. Open structure of double-stranded telomeric repeats bound by a multiprotein complex known as 'shelterin' or the 'telosome', containing telomere binding factors TRF1 and TRF2, TIN2 (TRF1-interacting nuclear factor 2), RAP1, POT1 and TPP1 (also known as POT1- and TIN2-organizing protein). (de Lange, 2005)

Fig.1.2.2. t and d-loop structure of telomere. T-loop and D-loop structure of mammalian telomeres hiding the free ends of telomeres in the loop structure. (Shay, 1999).

1.3. Telomerase and its function.

When telomeres reach a critically short length where it cannot form a protective t-loop, the cells undergo replicative stress and finally enter a stage of permanent cell cycle arrest known as "replicative senescence" (Allsopp et al., 1995; Allsopp and Harley, 1995; Hayflick, 1965). To compensate for telomere shortening an enzyme complex exists that can synthesize telomere de novo. This enzyme is called "telomerase". Telomerase is a heterodimer which is composed of a RNA component TERC (Telomerase RNA Component) and a catalytic protein component TERT (Telomerase Reverse transcriptase)(Greider and Blackburn, 1989; Meyerson et al., 1997). In humans, telomerase expression is tightly regulated and it is active only during embryogenesis. Telomerase activity is suppressed postnatally in most of the somatic tissues except in stem cell compartment and also in germ cell compartment (Chiu et al., 1996; Wright et al., 1996). The telomerase gene was mapped to 5p15.33 as one of the most distal genes on chromosome 5p (Shay and Wright, 2000).

 It is estimated that human telomeres lose about 50-100 base pairs from their telomeric DNA after each round of replication (Lundblad, 1997). This represents about 10-15 TTAGGG repeats. In cells with active telomerase and as it mimics the reverse transcriptase, it recognises TTAGGG repeats and elongates the hanging 3' parental fragment by using its own RNA as a complementary primer. Replication of the lagging strand can now be completed using the telomeric extensions as a template for synthesis using telomerase (Blackburn, 1997)
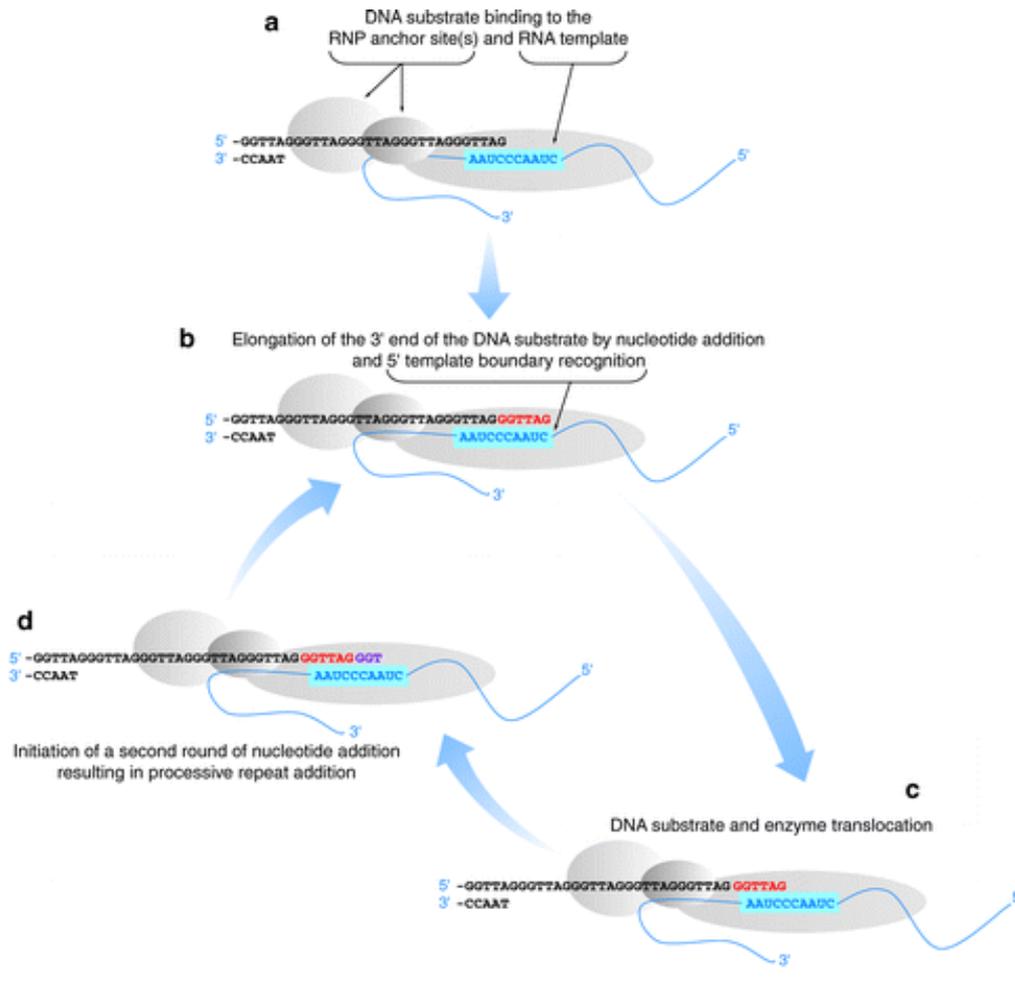
Fig.1.3.1. **Function of telomeres**. Model for processive elongation of telomeres by telomerase. The figure shows how telomerase enzyme elongates the telomeres using its Terc and Tert components.(Autexier and Lue, 2006)

Cells which lack telomerase enzyme, due to the above mentioned end replication problem the telomeric DNA looses its telomeric repeats over each round of cell division and finally become too short such that they cannot form the t-loop. The opened telomeric DNA with free ends will be recognised as DNA breaks and this induces DNA damage signals involving the p53 pathway. Activation of p53 induces cell proliferation arrest in cells with dysfunctional telomeres. This arrest is permanent and is termed "replicative senescence". It is also known as mortality stage, `M1` (Wright and Shay, 1992). If cells lose p53 checkpoint function they can bypass the M1 checkpoint and continue to proliferate despite telomere dysfunction leading to further telomere shortening and to an increase in the level of telomere dysfunction. This accumulation of telomere dysfunction induces massive levels of chromosomal instability leading to cell death. Cell death at this stage is p53independent and the checkpoint has been termed crisis or mortality stage `M2` ´(Wright and Shay, 1992).

Cell Division
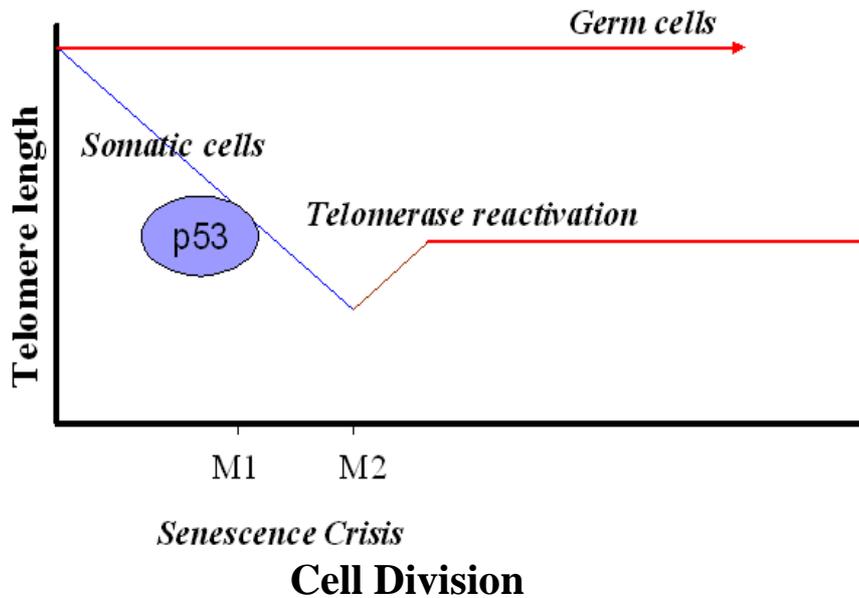
Fig.1.3.2. Classical M1 and M2 model. The figure shows p53 dependent cell cycle arrest due to telomere shortening in somatic cells where telomerase is absent and cells with active telomerase and lack p53 dependent checkpoint escapes the crisis stage and grows indefinitely. (Hayflick, 1965).

1.4. DNA damage signalling pathway.

In mammalian cells, DNA damage is a common problem which may cause cancer or ageing. DNA damage induces several responses including checkpoint activation and DNA repair. DNA damage checkpoints induce cell cycle arrest or apoptotic pathways if the level of DNA damage is too high or un repairable (Niida and Nakanishi, 2006). Two different types of DNA damage exists. The first one is the single strand DNA (ssDNA) damage and the other one is the double strand DNA (dsDNA) damage. For example, ssDNA damage is caused by Ultraviolet (UV) irradiation, which can cause dimerization of adjacent pyramidines in DNA, which causes saviour obstacle to DNA transcription and replication (de Laat et al., 1999). In contrast, dsDNA damage is caused internally by reactive oxygen species formed as intermediates in the oxidative metabolism (Featherstone and Jackson, 1999) of a cell or when replication fork stalls at the sites of DNA damage (Greider, 1991) and externally by ionising radiation (IR). In yeast the main mechanism for dsDNA damage repair is the homologous recombination (HR) and in mammals' the repair occurs by the non-homologous end joining (NHEJ) mechanism (Featherstone and Jackson, 1999).

One of the main responses of a cell to DNA damage is to delay or arrest the cell cycle by activation of DNA damage checkpoints (Abraham, 2001; Lowndes and Murguia, 2000). The first step in the initiation of DNA damage checkpoints is the recognition of DNA

damage. When DNA damage occurs, the following proteins will be activated: Rad9, Rad1 and Hus1. These 3 proteins interact together under the regulation of Rad 17 to form a Complex known as "9-1-1 complex" and bind to the site of DNA damage and initiates the DNA damage signalling cascade (Kondo et al., 2001; Melo et al., 2001).

1.4.1. ATM and ATR, the central protein kinases in the DNA damage response.

After the initiation of the DNA damage signal, the signal will be further amplified by either ATM (ataxia telangiectasia mutated) or ATR (ataxia telangiectasia and Rad-3-related) depending on the type of the DNA damage. Both protein kinases (ATM and ATR) belong to a family of protein kinases namely PIKKs (phosphatidyl inositol 3-kinase–like protein kinases). ATR plays a central role in regulation of a broad range of DNA damage signalling such as for formation of pyrimidine dimers, stalled replication forks and also regulates the responses towards ssDNA formed during the processing of DNA double strand breaks (Zhou and Elledge, 2000; Zou and Elledge, 2003). Unlike ATR, ATM is more specific in regulating the DNA damage signalling to DNA double strand breaks (DSBs) (Nyberg et al., 2002). Disruption of *ATR* at organismal level is embryonic lethal and the *ATR* knockout embryos die at day 7.5 postcoitum (Brown and Baltimore, 2000). On the other hand *ATM* knock out mice are viable but are growth retarded, infertile, radiosensitive and show severe immune defects (Barlow et al., 1996). In humans, mutations in *ATM* cause a rare autosomal recessive disorder known as "Ataxia telangiectesia" which is characterised by degeneration of the cerebellum, immunodeficiency, genome instability, clinical radiosensitivity and predisposition to cancer (Shiloh, 1997). It has been proved that in response to DSBs, ATR also phosphorylates some targets of ATM which plays a role in the induction of DNA damage signals (Jazayeri et al., 2006).

1.4.2. ATM mediated DNA damage signalling.

In the absence of DNA damage ATM exists as a homodimer in which the kinase domain is physically blocked by tight intermolecular binding to a protein domain at around Ser1981. DSBs in DNA causes a conformational change in the ATM protein that stimulates the kinase domain to phosphorylate Ser1981 by intermolecular autophosphorylation, resulting in dissociation of the homodimer (Bakkenist and Kastan, 2003). This phospho-ATM is the active form of ATM which then phosphorylates and activates its downstream cell cycle checkpoint proteins such as H2AX, CHK2, p53 etc to amplify the initial DNA damage signal to halt the cell cycle until the damage is repaired. Recently it has been demonstrated that

MRN (MRE11, RAD50, and NBS1) stimulates the kinase activity of ATM in vitro towards its substrates like histone H2AX, CHK2 and p53. MRN makes multiple contacts with ATM and appears to stimulate ATM activity by facilitating the stable binding of substrates (Lee and Paull, 2004). In addition to activating ATM, the MRN complex is also involved in maintaining the telomere structure intact together with TRF2 (Zhu et al., 2000; Verdun et al., 2005). After ATM phosphorylation by MRN complex, ATM then phosphorylates H2AX on the residue serine 139 (Rogakou et al., 1998). Phosphorylation of H2AX at serine 139 to γH2AX is required for the accumulation of numerous essential proteins at the site of DNA damage to amplify the DNA damage signal.

Now a days γH2AX is being used as a marker to identify the sites of DNA damage (Paull et al., 2000). Once H2AX is phosphorylated to γH2AX, the signal will be passed to NBS1 which phosphorylates and further amplifies the signal by passing the signal to the next down stream checkpoint protein CHK2 through 53BP1 (Celeste et al., 2003; Ward et al., 2003). CHK2 is activated by phosphorylation of its ´threonine´ residue at position 68 in ATM dependent manner in response to DSB´s (Buscemi et al., 2001). The exact role of CHK2 was established by examining *CHK2* knock out mice, which revealed that CHK2 is mainly involved in inducing p53 mediated apoptosis in response to DSB´s. The rate of apoptosis mainly depend on the level of DSB´s in the cell (Melchionna et al., 2000). After the activation of CHK2, CHK2 phosphorylates CDC25A, which is required for S phase entry (Melo et al., 2001), as well as CDC25 C, which is necessary for G2/M checkpoint (Takai et al., 2002). It has been shown that CHK2 also plays a role in inducing replicative senescence in response to telomere shortening in primary human fibroblasts (Hoffmann et al., 1994; Gire et al., 2004).

1.4.3. Role of p53 in response to DNA damage and senescence.

p53 is a tumor suppressor protein which plays a crucial role in the cells decision to induce either cell cycle arrest or apoptosis in response to different types of DNA damage (Brown et al., 1999; Gire et al., 2004). When DNA damage occurs, p53 is phosophorylated at different sites inducing either senescence or apoptosis. ATM phosphorylates p53 at Ser15 (Ser 18 in murines (Sluss et al., 2004)) which inhibits its interaction with MDM2 (Mouse double minute 2). MDM2 mediates p53 degradation when there is no DNA damage. CHK2 phosphorylates p53 at Ser20 in response to DNA damage , which also stabilises p53 from degradation by reducing its contact with MDM2 (Banin et al., 1998; Chehab et al., 1999; Chin

et al., 1999; Giaccia and Kastan, 1998; Shieh et al., 1997). p53 can induce cell cycle arrest at G1/S stage and G2/M stage of the cell cycle in response to DNA damage. p53 induces a G1 cell cycle arrest in response to DNA damage and telomere dysfunction by inducing the expression of a cyclin dependent kinase inhibitor (CDKI) known as p21 (el Deiry et al., 1993; Brown et al., 1997). p21 inhibits cyclin-E (Harper et al., 1993), which is necessary for G1/S transition. p21 also inhibits cyclin-D, which can phosphorylate RB (Retinoblastoma). RB is a potential regulator of the transcriptional factor E2F. E2F remains inactive when it is bound to pRB. Upon Rb phosphorylation E2F dissociates from pRB and then activates a set of genes required for G1/S transition of the cell cycle (Maiti et al., 2005). Together, p21 is an important downstream target of p53 inducing G1 cell cycle arrest in response to various kinds of DNA damage. It has been shown that DNA damage signals in response to telomere dysfunction are very similar to signals induced by DNA double strand breaks (d'Adda et al., 2003; Herbig et al., 2004). Further work showed that dysfunctional telomeres are detected as DNA damage in the G2 phase of the cell cycle (Verdun et al., 2005). It has been recently identified that senescing human cells and ageing mice accumulates unrepairable DNA lesions with double strand breaks throughout the genome (Sedelnikova et al., 2004). Some studies reveal that telomere shortening induces lot of stress in a cell which leads to increased production of ROS and this ROS in turn increases the rate of telomere shortening and also create more damage to the DNA (von Zglinicki et al., 2001). All types of DNA damage co-operate together and take the cell to its final destination either to so called 'senescence' or 'apoptosis'.
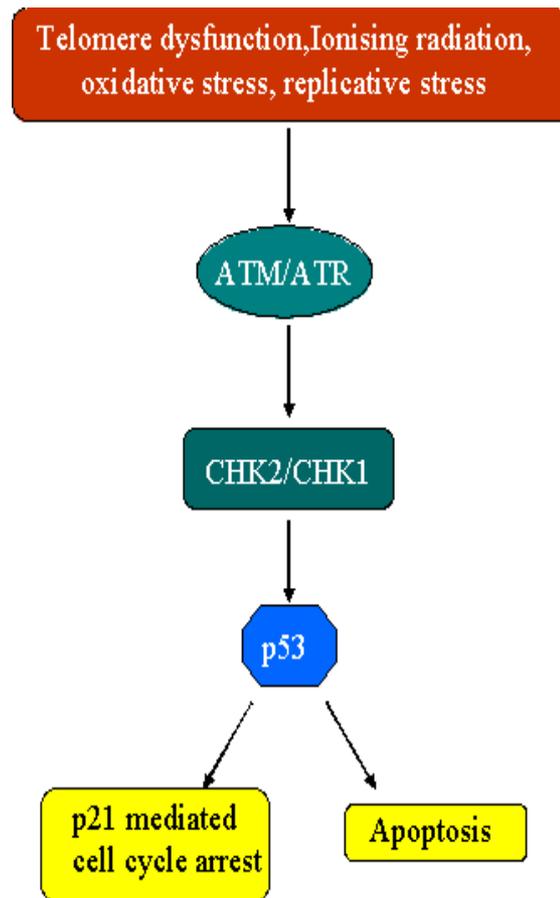
Fig-1.4.DNA damage signalling in response to dysfunctional telomeres and various kinds of DNA damaging agents.

1.5. Different roles of different DNA damage checkpoint proteins in response to telomere dysfunction in telomerase RNA component (mTerc) knockout mouse.

To see the effect of telomerase loss Blasco *et al* in 1997 produced a mouse model which lacks telomerase RNA component (mTerc). In the first generation of *mTerc*$^{-/-}$ mouse didn´t exhibit any abnormal phenotype showing that telomerase is not essential for the embryogenesis and development of the mouse due to very long telomere reserves in the laboratory mice (Blasco et al., 1997). However when *mTerc*$^{-/-}$ mice were further crossed, the first generation (G1) *mTerc*$^{-/-}$ mice produced second generation (G2) *mTerc*$^{-/-}$ mice and so on until the third to sixth generation (G3 to G6) depending on the mouse strain used. Late generation of mTerc-/- mice have critically short telomeres and show an accumulation of dysfunctional telomeres and chromosome fusions. These mice exhibit a loss of spermatogonia due to apoptosis resulting sterility of the mice. In addition, the mice show proliferative defects and increase in apoptosis in various high turnover organs including spleen and intestinal epithelium (Lee et al., 1998a; Rudolph et al., 1999).

To reveal the roles of DNA damage checkpoints in the context of telomere dysfunction, studies were performed on double mutants e.g. $mTerc^{-/-}ATM^{-/-}$, $mTerc^{-/-}p53^{-/-}$, $mTerc^{-/-}p21^{-/-}$ and $mTerc^{-/-}Ink4a$.

Studies on telomere dysfunctional mice with deletion of different components (genes) of the DNA damage pathway have shown different effects on organ homeostasis, cancer and lifespan of telomere dysfunctional mice depending on the level at which the DNA damage pathway was disrupted. Deletion of ATM increased telomere dysfunction and accelerated premature ageing of $mTerc^{-/-}$ mice, but telomere dysfunction suppressed the formation of lymphoma associated with ATM deletion (Qi et al., 2003; Wang and Zhu, 2003). ATM deletion did not rescue premature ageing phenotypes of telomere dysfunctional mice. But, the deletion of p53 rescued germ cell apoptosis of telomere dysfunctional mice. This rescue was associated with improved fertility in late generation $mTerc^{-/-}$ mice (Chin et al., 1999). However, p53 deletion did not improve lifespan of telomere dysfunctional mice due to an increase in cancer formation (Artandi et al., 2000). In contrast to the deletion of p53, the deletion of the $Ink4a$ gene locus did not rescue tissue atrophy in $mTerc^{-/-}$ mice, but telomere dysfunction suppressed tumor formation associated with Ink4a deletion (Greenberg et al., 1998).

The deletion of p21, a downstream target of p53, improved stem cell function, organ maintenance and lifespan of telomere dysfunctional mice without accelerating cancer formation. In these mice, p21 deletion rescued cell cycle arrest in intestinal progenitor cells and the depletion of hematopoietic stem cells, but p21 deletion left apoptotic responses intact (Choudhury et al., 2007).

Together, these results indicate that on one hand the induction of DNA damage signals limits stem cell function and organ homeostasis in response to telomere dysfunction and ageing and on the other hand, especially when p53 function is compromised, telomere dysfunction can lead to chromosomal instability and increase in tumor initiation (Artandi et al., 2000; Chin et al., 1999).

1.6. $Rad50^{s/s}$ mouse model.

The $Rad50^{s/s}$ mice are derived from the $Rad50$ locus with a change of a nucleotide AAG to ATG in exon1 resulting in the change of amino acid K to M at position 22. These mice die earlier at 4-5 months of age due to severe haematopoietic failure and will be apparent by the age of 4-8 weeks (Bender et al., 2002). These mice show hyper activation of DNA damage checkpoint signalling, which is mediated by ATM. Double mutant mice

generated by crossing *Rad50*[s/s] with *ATM* or *Chk*2 deficient mice showed a rescue in the survival as well as improved haematopoiesis as compared to Rad50ss mice wild type ATM or CHK2. These data confirmed that RAD50 acts very upstream in the DNA damage signalling cascade activating ATM and CHK2 signalling (Morales et al., 2005).

1.7. *53BP1* mouse model.

As mentioned earlier, 53BP1 is an upstream DNA damage checkpoint protein to CHK2 in the double strand DNA damage signalling pathway. The 53BP1deficient mouse was generated by replacing the exon from nucleotides 3777 to 4048 of mouse 53BP1 cDNA with PGK-neo[r] gene. These mice show weight loss when compared to normal wild type mice as they grow older and are radiosensitive. MEF´s derived from *53BP1*^{-/-} showed impaired activation of CHK2 at low dose of γ-irradiation (4Gy) and at high doses showed no impairment of CHK2 activation suggesting that 53BP1 is required for optimal activation CHK2 at low doses of IR (Ward et al., 2003).

1.8. *Exo1* mouse model.

Eukaryotes have nearly 15 different DNA polymerases which are involved in maintaining the fidelity of the DNA during the process of replication. Among all these 15 polymerases DNA polymerase γ, δ and ε are the most important as these have the ability of proof-reading activity during DNA replication because they have both $3'$-$5'$ and $5'$-$3'$ exonuclease activity (Hubscher et al., 2002). Exo1 has $5'$-$3'$ exonuclease activity and is one of the components of DNA polymerase 'δ'. Knockout mice carrying a deletion mutation of the nuclease domain of Exo1 are viable, but show defects in DNA mismatch repair accompanied with a slight increase in cancer susceptibility at advanced age (Wei et al., 2003).

A functional role of Exonuclease-1 (EXO1) for the induction of checkpoints in response to telomere dysfunction has been revealed in studies on yeast. Deletion of *Exo1* rescued the induction of senescence in telomere dysfunctional yeast strains. Exo1 can also mediate survival of telomere dysfunctional yeast strains by increasing homologous recombination at dysfunctional telomeres (Maringele and Lydall, 2004). In addition, EXO1 processing of dysfunctional telomere has been implicated in generating chromosomal translocation in response to telomere dysfunction (Hackett and Greider, 2003). Defects in mismatch repair have been shown to promote telomerase-independent proliferation in yeast (Rizki and Lundblad 2001).

Work from Dr. Sonja Schaetzlein in our group has shown that Exo1 deletion prolonged survival of G3 mTerc$^{-/-}$ mice. This elongated survival was associated with impaired cell cycle arrest and a reduction in apoptosis in G3*mTerc*$^{-/-}$ *Exo1*$^{-/-}$ double knockout mice compared to G3*mTerc*$^{-/-}$ *Exo1*$^{+/+}$ mice (Schaetzlein et al., 2007).

1.9. Summary and the focus of the current study

It is unknown, whether EXO1 has a role in initiating DNA damage response to telomere dysfunction or extra-telomeric DNA breaks in mammalian cells. The main aim of my study was to check whether Exo1 is required for the initiation of DNA damage signals in response to telomere dysfunction and γ-irradiation. To this end, I analyzed the influence of Exo1 gene status on DNA damage signalling in response to telomere dysfunction and irradiation in mice.

It is already known that RAD50 is an upstream signalling protein in dsDNA damage signalling pathway. With the study on *53BP1* and *Rad50*^{ss} double mutants we checked whether 53BP1 is either upstream or down stream to RAD50 in the DNA damage signalling pathway.

2. Materials and methods

2.1. Antibodies

7AAD	BD pharmingen
53BP1	Cell signalling
Actin	Santa Cruz
Annexin V-PE conjugated	BD Pharmingen
Anti-Mouse BrdU antibody	Amersham
Anti-mouse BrdU antibody	BD pharmingen
ATR	Cell Signalling
B220-Fitc conjugate anti-mouse	BD Pharmingen
B220-PE conjugate anti-mouse	BD Pharmingen
CD4-Fitc conjugated anti-mouse	BD Pharmingen
CD8-APC conjugated anti-mouse	BD Pharmingen
CD11b-APC conjugated anti-mouse	BD Pharmingen
CD11c-PercP conjugated anti-mouse	BD Pharmingen
CD43-biotinylated anti-mouse	BD Pharmingen
cKit-APC conjugated	BD Pharmingen
Cy3-conjugated Goat anti-Mouse	Zymed
FITC-conjugated anti-goat	BD Pharmingen
FITC-conjugated Goat anti-Mouse	Zymed
FITC-conjugated Goat anti-rabbit	Jackson Laboratories
γH2AX	Upstate
HRP conjugated anti-mouse	Zymed
HRP conjugated anti-rabbit	Zymed
IgD FITC conjugated anti-mouse	BD Pharmingen
IgM APC conjugated anti-mouse	BD Pharmingen
p21	Santa Cruz
p53	R&D Systems
p53	Vector Labs
pChk2-T68	Abcam
Peroxidase anti-mouse IgG2a	Amersham
Rad50	Bethyl Laboratories
Telomere probe Cy3-OO-(CCCTAA)$_3$	Applied Biosystems

2.2. Cell culture reagents

Advanced DMEM F12	Gibco
L-Glutamine	Gibco
New born Calf Serum (NCS)	Sigma
Pencillin/Streptomycin	Gibco
Trypsin/EDTA solution	Biochrom

2.3. Chemicals

Agarose (Electrophoresis grade)	Gibco
Aquatex (water based mounting medium)	Merck
Ammonium chloride	Sigma
Ammonium persulphate	Fluka
5'-bromo-2'-deoxyuridine (BrdU)	Amersham
Bromophenol blue	Serva
BSA (bovine serum albumin)	PAA
Chemiluminescence reagent	Perkin elmer
Collagenase A	Sigma
Complete mini (protein stabiliser)	Roche
Chloroform	J.T.Baker
Citric acid	Merck
3, 3'-diaminobenzidine tetra-hydrochloride (DAB)	Roche
Deoxycholic acid	Applichem
dNTP´s	Invitrogen
EDTA (N, N, N', N'-Ethylenediaminotetraacetate)	Sigma
Ethanol	J.T.Baker
Ethidiumbromide	Sigma
Formaldehyde	Merck
Hemalum solution	Merck
Hydrochloric acid	Merck
Hydrogen peroxide	Merck
Isopropanol	J.T.Baker
Kanamycin	Sigma
Mayer´s Haematoxylin solution	Sigma
Methanol	J.T.Baker
Mounting medium for fluorescence	Vectashield

Mounting medium with DAPI	Vectashield
NNN´N´ tetramethylethylenediamine (TEMED)	Sigma
Paraformaldehyde	Merck
PBS (phosphate buffered saline)	PAA
Potassium bicarbonate	Sigma
Propidium Iodide	Sigma
Roti-Phenol/Chloroform	Roth
Sodium hydroxide	Merck
Sodium chloride	Merck
Sodium dodecylsulphate (SDS)	Sigma
Tris (Tris-(hydroxymethyl)-aminomethane)	Applichem
Tween 20	Sigma
Triton 100	Sigma

2.4. Enzymes, DNA ladder and Protein ladder

Proteinase K	Invitrogen
Pepsin	Sigma
RNase A	Sigma
Taq DNA polymerase-Go taq	Promega
DNA marker-1kb ladder	Life technologies
Precision plus protein ladder (Dual color)	Biorad

2.5. Laboratory equipment

0.20µm filter	Nalgene
0.45µM PVDF membrane	Millipore
22mm cover slips	Menzel-Glaser
24 x 50mm cover slips	Menzel-Glaser
76 x 26mm SuperFrost plus – Glass Slides	Menzel-Glaser
Abc (animal blood counter)	Scil animal care company
Chemiluminescence Film	Amersham
Desktop centrifuge	Eppendorf
Electrophoresis-Apparatus	Labtech,Pharmacia Biotech
Electrophoresis apparatus for PAGE	Bio-Rad
FACS (FACScan)	Beckton Dickinson

FACS tubes	Falcon
Fluorescence microscope	Olympus
Gel doc	Syngene
Heat block	Eppendorf
Hyper cassette	Amersham
Microscope	Olympus
Microscope equipped camera	Olympus
Microtome	Leica
Neubaur chamber	Marienfeld
Nylon net (60µm)	Fishcher scientific
PCR master cycler	Eppendorf
PCR soft tubes	Biozym
Power-Supply	Biometra
Spectrophotometer	Eppendorf
Vortex	Omnilab
Western blotting chamber	Biorad

2.6. Kits

Annexin V-PE Apoptosis detection kit	BD pharmingen
Cell proliferation kit	Amersham
In situ cell death detection kit	Roche

2.7. Mouse crosses and survival.

2.7.1. *mTerc* and *Exo1* colony.

Exo1$^{+/-}$ mice were crossed with $mTerc^{+/-}$ mice to generate $mTerc^{+/-}$, $Exo1^{+/-}$ mice. These mice were crossed through successive generations to produce G3 mTerc$^{-/-}$Exo1$^{+/+}$ and G3$Exo1^{-/-}$ mice. Intercrosses between $mTerc^{+/+}Exo1^{+/-}$ generated $mTerc^{+/+}Exo1^{+/+}$ and $mTerc^{+/+}Exo1^{-/-}$ mice. Mice were maintained on a C57BL/6J background. Mice were monitored by one inspection per week (Work from Sonja Schaetzlein).

2.7.2. *Rad50* and *Exo1* colony.

$Rad50^{+/+}Exo1^{+/-}$ mice were crossed with $Rad50^{s/+}Exo1^{+/+}$ mice to generate $Rad50^{s/+}$, $Exo1^{+/-}$mice. These mice were crossed with each other to generate $Rad50^{s/+}Exo1^{+/-}$. These double heterozygotes were crossed with each other to generate $Rad50^{s/s}Exo1^{-/-}$in a mixed background of C57BL/6J and 129/SvEv. Mice were monitored by one inspection per week.

2.7.3. *Rad50* and *53BP1* colony.

$53BP1^{+/-}$ mice were crossed with $Rad50^{s/+}$ mice to generate $Rad50^{s/+}53BP1^{+/-}$ mice. These mice were crossed with each other to generate $Rad50^{s/+}$, $53BP1^{+/-}$. These double heterozygotes were crossed with each other to generate $Rad50^{s/s}53BP1^{-/-}$ in a mixed background of C57BL/6J and 129/SvEv.

The mice were bred and maintained in the animal facility, Medical School, Hannover, on a standard diet and in 14 hrs of light and 10 hrs of dark periods. Mice were monitored by one inspection per week.

2.8. Molecular methods.

2.8.1. DNA Extraction from mouse tails.

$Exo1^{+/+}$, $Exo1^{-/-}$, $Rad50^{s/s}$, $Rad50^{s/s}Exo1^{-/-}$, $53BP1^{+/+}$, $53BP1^{-/-}$, $Rad50^{s/s}53BP1^{-/-}$ mice were identified from the mouse colony by PCR amplification method. The DNA was extracted from the mice tails by standard Phenol-Chloroform method. In brief, a small piece of tissue was cut from the tip of the mouse tail and digested in 500µl of lysis buffer (10mM NaCl + 10mM Tris-HCl (pH 8.0) + 25mM EDTA pH 8.0 + 0.5% SDS; 64µl of proteinase K was added to 10ml of this buffer) overnight with continuous shaking at 56ºC. Then 1ml of phenol/chloroform was added continuously but gently shaken for 1 min at room temperature and centrifuged at 10,000rpm for 5 min. The supernatant was collected and 1ml of chloroform was added and continuously shaken for 10 min at room temperature and centrifuged for 5 min

at 10,000rpm. To the supernatant, 1ml of iso-propanol was added (DNA precipitation) and gently shaken by inverting the eppendorf tube for 1 min and then centrifuged at 13,000rpm for 10 min. The supernatant was discarded and the DNA pellet was washed twice with 70% ethanol and centrifuged at 13,000rpm for 5 min. The DNA pellet was air dried for 5 min and dissolved in 50µl of TE buffer (10mM Tris-HCl (pH 7.6), 10mM EDTA).

Primers and the reaction conditions used for genotyping are as follows:

2.8.2. Genotyping for *mTerc* mice:

mTRR-5'-TTCTGACCACCACCTACTTCAAT-3',

5ppgK-5'-GGGC TGCTAAAGCGCAT-3',

mTRwtF-5'-CTAAGCCGGCACTCCTTACAAG-3'.

(1µg of DNA + 2.5µl 10X PCR buffer + 1.5µl 3mM MgCl2 + 0.5µl dNTP's + 1.0 µl mTRR primer (10 pmol) + 1.0µl 5ppgK primer (10 pmol) + 1.0µl mTRwtF primer (10 pmol) + 0.25µl Taq DNA polymerase + 15.25µl dH$_2$O). The PCR cycle profile is as follows: initial denaturation at 94ºC for 30 sec, annealing at 55ºC for 30 sec, and extension at 72ºC for 30 sec. Thirty cycles of PCR amplification were performed and the PCR products were run on 2% agarose gel and visualized with ethidium bromide (25µl of 1mg/ml conc. for 100ml of agarose gel). The primers amplify a fragment of 250 bp for $mTerc^{+/+}$ and 180 bp for $mTerc^{-/-}$ and both the fragments for $mTerc^{+/-}$ **.**

2.8.3. Genotyping for *Exo1* mice:

Primer A - 5'-CTT CGC TTT ATG AAG CAG CC -3',

Primer B -5'-AGG AGT AGA AGT GGC GCG AAG G -3',

Primer C-5'-AGG AAA GAG TCA GAG TGC TGG C-3'.

(1µg of DNA + 10µl 5X PCR buffer + 5µl 25mM MgCl$_2$ + 0.5µl dNTP's + 0.75µl primer A (10 pmol) + 1.0µl primer B (10 pmol) + 1.25µl primer B (10 pmol) + 0.20µl Taq DNA polymerase + 29.3µl dH$_2$O). The PCR cycle profile is as follows: initial activation at 94ºC for 5 min, 94°C for 0.45 min, annealing at 55ºC for 1 min, and extension at 72ºC for 1 min. Forty cycles of PCR amplification were performed, finally additional extension at 72°C for 5 min and the PCR products were run on 2.5% agarose gel and visualized with ethidium bromide (25µl of 1mg/ml conc. for 100ml of agarose gel). The primers amplify a fragment of 349 bp for $Exo1^{+/+}$ and 318 bp for $Exo1^{-/-}$ and both the fragments for $Exo1^{+/-}$.

2.8.4. Genotyping for *Rad50* mice:

Rad50 WT - 5'-GCC TAT GTA AGC ATT AAC TAG CAA CA -3',

Rad50 CP -5'-GGA GTC CTA AGC AAC ACG AGC -3',

Rad50 Mut -5'-CCT ACC CGC TTC CAT TGC TCA-3'.

(1µg of DNA + 1µl 5X PCR buffer + 2µl 25mM MgCl$_2$ + 0.25µl dNTP's + 1µl Rad50 WT (10 pmol) + 1.0µl of Rad50 CP (10 pmol) + 1 µl of Rad50 Mut (10 pmol) + 0.25µl Taq DNA polymerase + 1.65µl dH$_2$O). The PCR cycle profile is as follows: initial activation at 94ºC for 3min, 94°C for 15 sec, annealing at 64ºC for 30 sec, and extension at 68ºC for 90 sec. Thirty five cycles of PCR amplification were performed, finally additional extension at 68°C for 5 min and the PCR products were run on 2% agarose gel and visualized with ethidium bromide (25µl of 1mg/ml conc. for 100ml of agarose gel). The primers amplify a fragment of 680 bp for *Rad50$^{s/s}$* and 520 bp for *Rad50$^{+/+}$* and both the fragments for *Rad50$^{+/s}$*.

2.8.5. Genotyping for *53BP1* mice:

Con4 4206F - 5'-CCT ACC CGC TTC CAT TGC TCA-3',

Con4 4478R -5'-CTC AGT TTT CCT GGG CCT CCT -3',

Neo 549F-5'-GAT CGG CCA TTG AAC AAG ATG-3' and

Neo 1004R -5'-GGC TTC CAT CCG AGT ACG TGC T-3'.

(1µg of DNA + 5µl 5X PCR buffer + 3µl 25mM MgCl$_2$ + 0.5µl dNTP's + 1µl Con4 4206F (10 pmol) + 1.0µl of Con4 4478R P (10 pmol) + 1µl of Neo 549F (10 pmol) + 1µl of Neo 1004R (10 pmol) +0.1µl Taq DNA polymerase + 10.4µl dH$_2$O). The PCR cycle profile is as follows: initial activation at 95ºC for 10min, 94ºC for 1 min, annealing at 51ºC for 1 min, and extension at 72ºC for 1 min. Twenty five cycles of PCR amplification were performed, finally additional extension at 72ºC for 6 min and the PCR products were run on 2% agarose gel and visualized with ethidium bromide (25µl of 1mg/ml conc. for 100ml of agarose gel). The primers amplify a fragment of 450 bp for *53BP1$^{-/-}$* and 270 bp for *53BP1$^{+/+}$* and both the fragments for *53BP1$^{+/-}$*.

2.8.6. Western blot.

2.8.6.1. Protein preparation. Whole cell extracts of mouse ear fibroblasts were obtained by resuspending the pellet in RIPA lysis buffer (50mM Tris-HCl (pH 8.0) 150mM Nacl, 1% NP-40, 0.5% deoxycholic acid, 0.1% SDS, 1mM Sodium meta vanadate, 1mM DTT, 1mM PMSF and finally protease inhibitor) for 20 minutes on ice and then centrifuged at 13,200rpm for 15

minutes and collected the supernatant. The protein was quantified by using adding Bio-Rad reagent to the protein (protein 5µl, distilled water 795µl and Bio rad reagent 200µl), incubated at room temperature for 10 minutes and measured OD at 595 nm in spectrophotometer (Before measuring the protein, a blank was set using 800µl water and 200µl Bio-Rad reagent).

Calculation of protein concentration

Amount of protein (µg/ml) = OD at 595nm x ε x 200

ε   =   excitation co-efficient of protein.

200   =   Dilution factor.

20µg of protein is treated with loading buffer (0.5MTris Hcl pH 6.8, SDS powder-640mg, 100% glycerol-3.2ml, ß-mercaptoethanol-1.6ml, bromophenol blue -0.001gm dissolved in distilled water 2.14ml) and heated at 95°C for 10 minutes.

2.8.6.2. Protein separation through SDS-PAGE and Western blotting.

Protein was subjected to SDS-PAGE (Acrylamid:bis acrylamide 30:0.8, 1.5M Tris pH.8.8, distilled water, 10% ammonium persulphate, TEMED, in 1x running buffer Tris, Glycine and SDS pH8.8 at 60V for 2-3hrs) and blotted on the PVDF membrane using semidry western transfer apparatus using western transfer buffer for 20-30 minutes at 25V, 300mA (Western transfer buffer - Glycine-2.9gms, Tris-5.8gms, SDS-0.37gms, methanol-200ml all of them made up to one litre with distilled water). After blotting the membrane was blocked in 5% milk powder in TBS-Tween (Tris, borate, saline and 0.1% Tween 20 pH 7.6) for 1 hour and then the required protein was detected using antibody against phospho ATR (1:1000 dilution, cell signalling), Phospho Chk2-T68 (1:1000, Abcam), phospho-p53-Ser15 (1:1000 dilution; Cell Signalling and against ß-Actin (1:1000 dilution, Santa Cruz) over night incubation at 4°C and used HRP conjuagated secondary antibodies (Anti rabbit 1:2000 dilution, Zymed, Anti-mouse 1:2000 dilution depending upon the host in which primary antibodies were raised) and then developed the membrane with chemiluminescence reagent on the Chemiluminescence films in the developing machine.

2.9. Immunohistochemsitry.

2.9.1. Apoptosis staining on intestinal crypts.

The rate of apoptosis was determined by TUNEL assay (In situ cell death detection kit, Roche, Mannheim, Germany) on 5 µm thick paraffin sections of small intestine of 3-4 months old Exo1$^{+/+}$ and Exo1$^{-/-}$ mice which were irradiated with 4Gy and 24 hrs later sacrificed. Sections were deparaffinized and rehydrated in series of ethanol and permeabilised in 1mM sodium citrate buffer by heating at boiling temperature for 5 minutes and then heating at sub-boiling temperature for 10 min and then allowed to cool down at RT for 40 minutes. After washing the slides, the slides were incubated with Proteinase K (15µg/ml) directly on the section for 30 min at RT and washed twice with PBS and were probed with TUNEL-mix (Roche). After incubation for 90 min at 37°C slides were washed twice with PBS, air dried, mounted with antifade + DAPI (1:1), covered with coverslips and observed under the microscope in 40 low power fields (400x).

2.9.2. BrdU staining on intestinal crypts.

3-4 months old Exo1$^{+/+}$ and Exo1$^{-/-}$ mice were irradiated with 4Gy and 22 hours later mice were injected with 5-bromodeoxyuridine (i.p. injection of BrdU 30 mg/kg body weight) and killed 2 hours later after BrdU injection. Immunostaining was performed on 4µm-thick paraffin sections of small intestine using the Cell Proliferation Kit (Amersham Biosciences) according to the manufacturer's instructions. In brief, sections were deparaffinized and rehydrated in series of ethanol and permeabilised in 1mM sodium citrate buffer by heating at boiling temperature for 5 minutes and then heating at sub-boiling temperature for 10 min and then allowed to cool down at RT for 40 minutes. The slides were then washed in PBS twice and incubated in 0.3% hydrogen peroxide in methanol for 20 minutes in order to block endogenous peroxidase activity and then the slides were again washed with PBS twice and added primary antibody 1:1000 dilution in antibody diluent with the DNase provided along with the kit and incubated for 1-2 hrs at room temperature and washed twice with PBS. The slides were then probed with anti-mouse secondary antibody 1:75 in the diluent provided along with kit and incubated for 45 minutes at room temperature. The slides were then washed with PBS twice and probed with DAB 1:10 dilution (Roche) in the substrate solution for 10-20 minutes, washed twice in distilled water and then counter stained with haematoxylin for 2-4 seconds and again washed twice or thrice with water and mounted with aquatex and

the number of BrdU positive cells per crypt were counted in 20x low power fields (200x) per mouse.

2.9.3. γH2AX, ATR, 53BP1, p53 and p21 stainings on intestinal crypts.

Immunofluorescence was performed on 4-µm-thick paraffin sections of small intestine. Sections were deparaffinized and rehydrated in series of ethanol and permeabilised in 1mM sodium citrate buffer by heating at boiling temperature for 5 minutes and then heating at sub-boiling temperature for 10 min and then allowed to cool down at RT for 40 minutes. The slides were then washed in PBS twice and incubated with primary antibody: γ-H2AX (UpState, 1:750 dilution), ATR (cell signalling, 1:100), 53BP1 (Cell signalling. 1:100), p53 (R&D, 1:50) and p21(Santa cruz, 1:50) either over night at 4°C or for 2 hours in humid chamber at room temperature. The slides were washed twice with PBS before treated with secondary antibody: γ-H2AX and p21: Anti mouse (1:200 and 1:100 respectively) Cy3-Zymed, 53BP1: Anti rabbit (1:150) Fitc-Zymed, p53: Anti goat (1:100) Fitc-BD Pharmingen, for 1 hour at RT and washed with PBS twice, air dried and mounted with Antifade + DAPI (1:1 ratio), covered with coverslip and observed under microscope.

The evaluation of γ-H2AX in the case of G3 and G3Exo$^{-/-}$ was made as the percent of positive crypts, to this end 20 low power fields (200x) per mouse was counted. Positive crypts showed positive nuclear staining in 2 or more nuclei per crypt and negative crypts did not show any nuclear staining. In the case of irradiated mice γ-H2AX was evaluated as the number of foci per nuclei and was counted in 100 high power fields (1000x) per mouse.

In the case of 53BP1 the evaluation was made as the number of positive foci per crypt in the setting of dysfunctional telomeres as well as in the case of irradiation. 53BP1 was counted in 100 high power fields (1000x) per mouse.

For ATR, p53 and p21 staining, the evaluation was made as the percent of positive crypts and was counted in 20 low power fields (200x) per mouse. Positive crypts showed positive nuclear staining in 2 or more nuclei per crypt. Negative crypts did not show any nuclear staining.

2.9.4. Co-staining of Telomere probe with γH2AX and 53BP1.

4µm-thick paraffin sections of small intestine were deparaffinised and rehydrated in series of ethanol and permeabilised in 1mM sodium citrate buffer by heating at boiling temperature for 5 minutes and then heating at sub-boiling temperature for 10 min and then allowed to cool down for 40 minutes. The slides were then washed in PBS twice, dehydrated

in ethanol series, air dried for 5 minutes and added telomere probe conjugated with CY3, denatured the DNA at 80°c for 3 minutes and then incubated in humid chamber for 2 hours at room temperature. The slides were again washed twice with PBS and incubated with primary antibody (γH2AX-UpState 1:750 dilution, 53BP1-Cell Signalling. 1:100 dilution) for 2 hours in humid chamber at room temperature. The slides were washed twice with PBS after primary antibody incubation and treated with secondary antibody (for γH2AX, anti-mouse FITC, BD Pharmingen, 1:200, 53BP1- anti rabbit (1:150) FITC-Zymed,) for 1 hour at RT and washed with PBS twice, air dried and mounted with Antifade + DAPI (1:1 ratio) to the sections, covered with cover slips and observed under the microscope in 100 high power fields (1000x).

2.9.5. Co-staining of TUNEL with γ-H2AX.

4µm-thick paraffin sections of small intestine were treated as described above and incubated with γ-H2AX (Upstate, 1:750) for 2 hours in humid chamber at RT. Slides were than washed twice with PBS before incubating with secondary antibody (anti mouse-Cy3, Zymed, 1:200) for 1 hour at RT. After washing, the slides were probed with TUNEL-mix (Roche). After incubation for 90 min at 37°C slides were washed twice with PBS, air dried, mounted with antifade + DAPI (1:1), covered with cover slips and observed under the microscope in 40 low power fields (400 x).

2.10. Stainings for FACS analysis.

Mice were sacrificed at the respective time points and bone marrow was flushed from both the hind limbs with sterile PBS and pelleted down. After RBC lysis (ammonium chloride-0.15M, potassium bicarbonate-10mM, EDTA-0.1mM) for 3minutes at room temperature the cells were spin down and re-suspended in 1ml staining medium (PBS with 2% FBS and 0.02% sodium azide). The cells were counted in Neubauer chamber and 1 million cells were used for B-cell and myeloid cell compartment staining and 3 million cells were used for analysing stem cell compartment. For B-cell staining the cells were pelleted down and re-suspended in 50µl staining medium and added antibodies conjugated with respective fluorescent colors (B220 PE conjugated, IgD-FITC conjugated, IgM-APC conjugated, CD43 biotinylated which is again stained with Streptavadin conjugated to PercP antibody) and took the cells for FACS. For myeloid cells CD11b APC conjugated antibody and for dendritic cells CD11c PE or FITC conjugated antibodies were used. For stem cells

staining, cells were first treated with biotinylated lineage antibodies (Gr-1, Mac-1, B220-1:300 dilution, Ter119, CD3-1:200 dilution, CD4, CD8, CD5 -1:300 dilution in staining medium) and incubated for 15 minutes on ice in dark and washed with staining medium and then added ckit antibody conjugated to APC and Sca1-FITC conjugated antibody and streptavadin linked PercP-Cy5.5 for all lineage antibodies. For Annexin staining after staining with B220 FITC conjugated, CD11b –APC conjugated for 15 minutes. The cells were washed and stained for apoptosis with Annexin V –PE conjugated 1:20 dilution and 7AAD (7AAD excludes dead cells) 1:20 dilution in binding buffer provided by the kit and incubated at room temperature for 15 minutes in dark and added 500µl of binding buffer and cells were took for FACS. After FACS the data was analysed with Flow.jo softwere.

Note- Unless other wise mentioned the dilution of the antibodies used is always 1:25 in staining medium.

2.11. Cell culture methods-

2.11.1. Preparation of Mouse ear fibroblasts. The ear was obtained form the upper part of one ear, rinsed twice with PBS containing kanamycin (100µg/ml) and minced in Advanced DMEM F12(GIBCO) with out any supplements, incubated at 37°C for 2-3 hrs in collagenase A (10µg/ml). After incubation make cell suspension with syringe and centrifuge at 1200rpm for 10 minutes and re-suspended in Advanced DMEM F12 with 10% NCS, 5x L-Glutamine and with 5× PenStrep overnight.. When the cells are confluent, split them to 1:3 and passaged so on. Cells were cultured at 3% oxygen, 5% carbon dioxide.

2.11.2. Proliferation assay on mouse ear fibroblasts. Mouse ear fibroblasts were seeded in 10cm dishes and grown over night. Then cells were irradiated with 15Gy irradiation and 24 hours later cells were trypsinised and fixed in 70% cold ethanol for analysis. BrdU (10mM) was added 3 hrs before harvesting the cells. BrdU staining was performed according to manufacturer's instructions using anti-BrdU antibody (BD pharmingen). In brief cells were trypsinised and fixed in 5 ml of ice-cold 70% ethanol by adding ethanol drop by drop while vortexing and then incubated on ice for 30 minutes. Then the cells were centrifuged at 1500rpm for 10 min at 4ºC and the supernatant was aspirated and the pellet was re-suspended in 1 ml of 2N HCl + 0.5% Triton-X100 (17.2 ml of conc. HCl and 0.5 ml of Triton-X100 in 82.3 ml of distilled water) at room temperature for 30 min and then centrifuged at 1500rpm for 10 min and the supernatant was aspirated and the pellet was re-suspended in 1 ml of 0.1M

NaB_4O_7, pH 8.5 and then centrifuged at 1500rpm for 10 min and re-suspended in 1ml of 0.5% Tween-20/1% BSA/PBS and the cell concentration was adjusted to achieve 1 x 10^6 cells/test. Then the cells were incubated with 20µl of Anti-BrdU 10^6 cells for 2 hrs at room temperature and then washed once in 1 ml of 0.5% Tween-20/1%BSA/PBS and centrifuged at 1500rpm for 10 min and re-suspended in 0.5 ml of PBS + 5 µg (final conc.) of PI + 10 µl of 10 mg/ml RNase A. Flow cytometric analysis was carried out with FACScan (Becton Dickinson) equipped with Cell Quest software. Data was analysed using flow jo software.

2.11.3. ATR staining on Mouse ear fibroblasts. Mouse ear fibroblasts were grown on cover slips and cells were fixed in 4% formaldehyde for 30 minutes after 2Gy irradiation. Cells were washed twice with PBS and permeabilised with 0.2% triton100x in PBS for 10 minutes and washed twice with PBS. Then cells were treated with ATR antibody (1:500 dilution, Cell signalling) in PBS with 1%BSA, 1%Tween 20 for 2 hours and washed twice with PBS and cells were probed with anti rabbit FITC conjugated secondary antibody in PBS with 1%BSA, 1%Tween 20 for 1 hour at room temperature, washed twice and mounted with DAPI and ATR foci positive cells were counted under 40 low power fields (400x). (positive cell is the one which has more than 3ATR foci per nuclei).

2.12. Statistical analysis.

Statistical analysis was done using Microsoft Excel and Graph Pad Prism software. Error bars indicates + or – standard deviation. Unpaired Students t-test was used to generate the ´p' values for the data sets. Survival curves were calculated using the method of Kaplan and Meier.

3. Results.

3.1. Role of EXO1 in telomere shortening and γ–irradiation induced DNA damage.

3.1.1. *Exo1* deletion prevents the activation of DNA damage signals in response to telomere dysfunction.

The induction of DNA damage signalling pathways is the molecular basis for activation of checkpoints in response to DNA damage. The formation of DNA damage foci represents the very upstream molecular events associated with DNA damage signal induction at dysfunctional telomeres (d'Adda et al., 2003) and also in response to γ-irradiation (Maser et al., 1997). DNA damage foci containing γH2AX (Figure 3.1.1.A and B) and 53BP1 (3.1.1.C and D) were detected in basal, intestinal crypts of 12-15 month old G3*mTerc*$^{-/-}$ mice but not in age-matched *mTerc*$^{+/+}$ mice.

3.1.1. A.

G3Exo1+/+	G3Exo1-/-	mTerc+/+Exo1+/+

| γH2AX	γH2AX	γH2AX
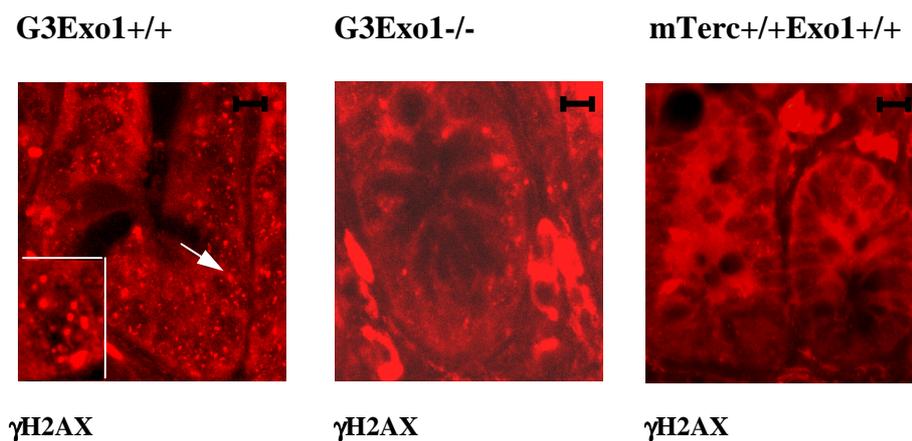
3.1.1.B.
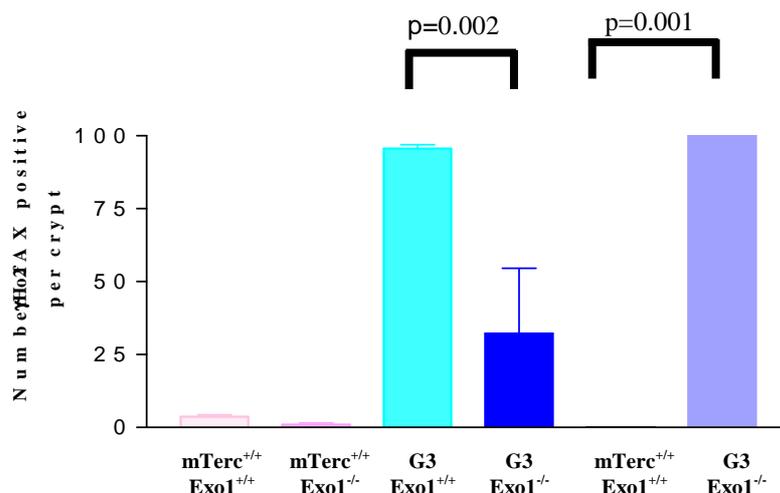
3.1.1.A. Representative photographs showing γ-H2AX positive cells (white arrows) in basal crypts of 12-15 month old mice of the indicated genotypes. Magnification bars 50µm. **B.** Histogram showing the percentage of γ-H2AX positive basal crypts in 12-15 and 24 month old mice of the indicated genotypes (n= 4-5 mice/group).

3.1.1.C

G3Exo1+/+　　　　**G3Exo1-/-**　　　　**mTerc+/+Exo1+/+**

53BP1　　　　　　53BP1　　　　　　53BP1
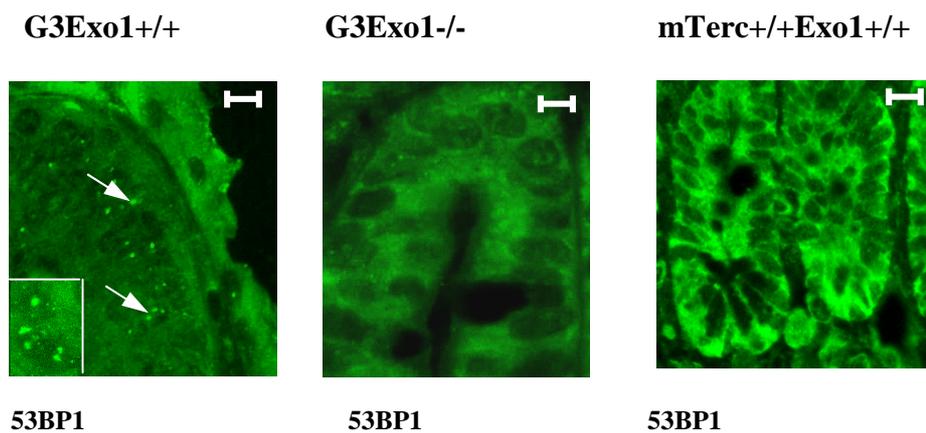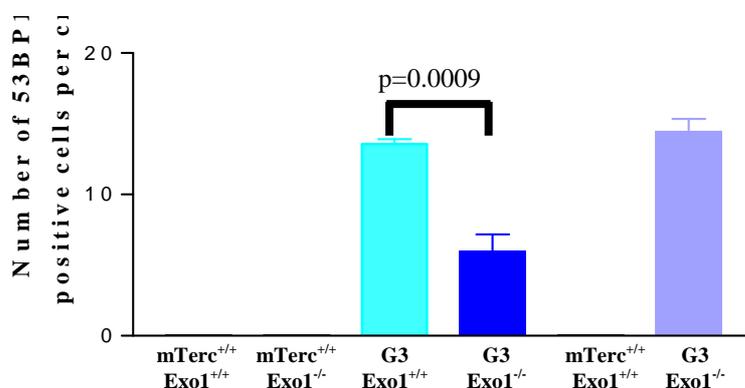
3.1.1. D.

3.1.1. D. Representative photographs showing 53BP1 positive cells (white arrows) in basal crypts of 12-15 month old mice of the indicated genotypes. Magnification bars 50µm. **F.** Histogram showing the percentage of 53BP1 positive basal crypts in 12-15 and 24 month old mice of the indicated genotypes (n= 4-5 mice/group).

Downstream DNA damage signaling in response to dysfunctional telomeres and DNA damage involves stabilization of p53 and the induction of p21 (Brown et al., 1999; Stein et al., 1999). We employed immunohistochemical analysis for p53 (3.1.1.E and F) and p21(Figure G) to assess whether this pathway was also perturbed in the G3$mTerc^{-/-}$, $Exo1^{-/-}$ mice. In 12-15 month old G3 $mTerc^{-/-}$, $Exo1^{+/+}$ mice nuclear expression of p53 was detected in 47% and p21 in 9.5% of basal intestinal crypts. p53 and p21 expression was not detected in mTerc$^{+/+}$ mice (n=4-5 mice per group). Both p53 and p21 up regulation was rescued in G3$mTerc^{-/-}Exo^{-/-}$ mice compared to G3 $mTerc^{-/-}$, $Exo^{+/+}$ mice (p<0.001).

3.1.1.E.

G3Exo1+/+	G3Exo1-/-	mTerc+/+Exo1+/+

p53	**p53**	**p53**
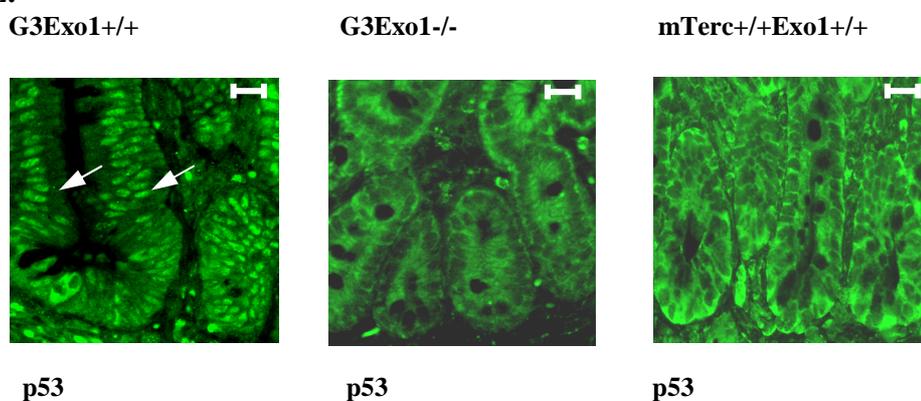
3.1.1.F.
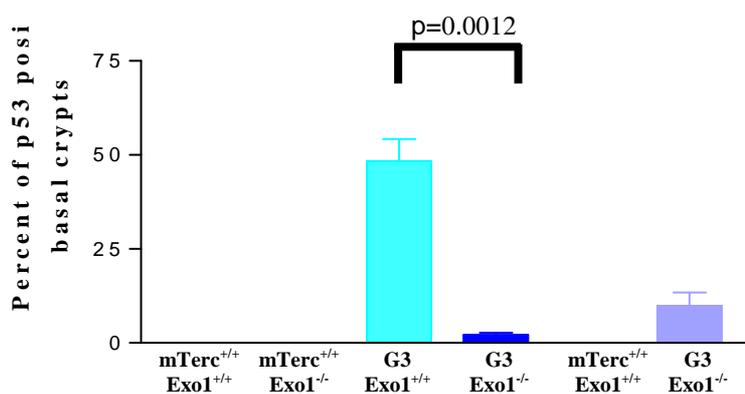
3.1.1.E. Representative photographs showing p53 positive cells (white arrows) in basal crypts of 12-15 month old mice of the indicated genotypes, magnification bars 200 µm. **F.** Histogram showing the percentage of p53 positive basal crypts in 12-15 and 24 month old mice of the indicated genotypes (n= 4-5 mice/group).

3.1.1.G.
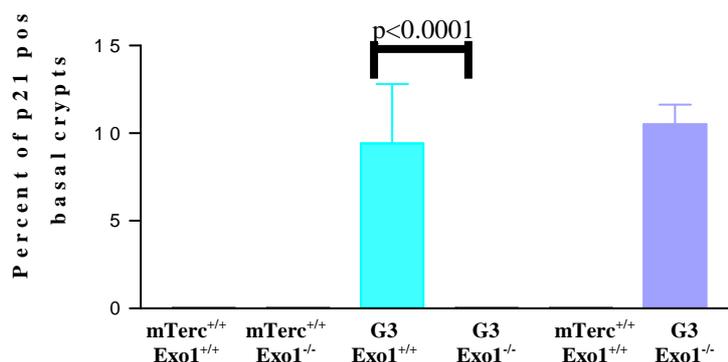
3.1.1.G. Histogram showing the percentage of p21-positive intestinal basal crypts of 12-15 and 25 month old mice of the indicated genotypes (n=4-5 mice/group).

To check wheather DNA damage foci formed in ageing G3mTerc$^{-/-}$ mice reflect apoptotic cells, we did co-staining of γH2AX with TUNEL-positive apoptotic cells (Figure 3.1.1.I) which revealed that DNA damage foci were present in non-apoptotic cells of ageing G3*mTerc*$^{-/-}$ mice indicating that the DNA-damage foci staining did not reflect DNA breaks in apoptotic cells.

3.1.1. I.
   TUNEL   **γH2AX**
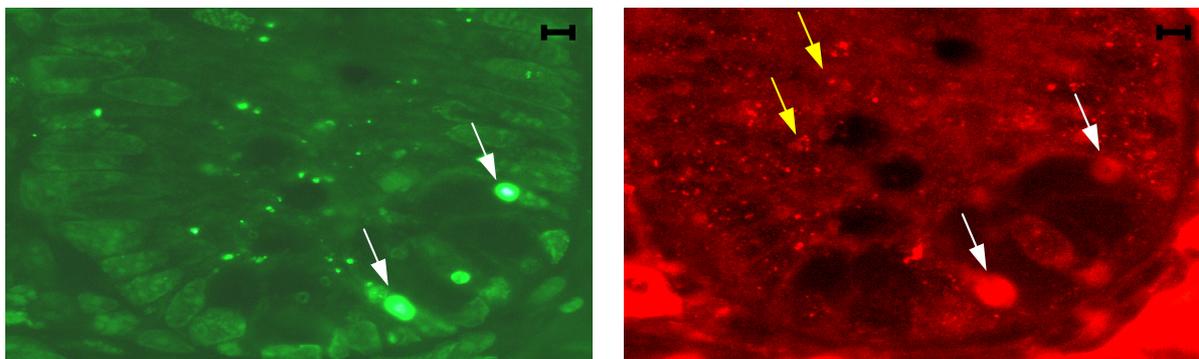
3.1.1. I. Representative photograph showing apoptotic nuclei (white arrows) and γ-H2AX -foci positive nuclei (yellow arrows) in basal crypts of a 12-15 month old mice. Note that the apoptotic nuclei do not co-localize with γ-H2AX-foci positive nuclei.

The data from Co-staining of γH2AX (3.1.1.J and 3.1.1.L) and 53BP1 (3.1.1.K) with Immuno-FISH revealed a co-localization of DNA damage foci with telomeric DNA in 14% of the total number of DNA damage foci. This number appears to be reasonable given the fact that DNA damage foci form at dysfunctional telomeres, which frequently lack detectable

telomeric sequence. In addition, it is possible that crypt cells with dysfunctional telomeres accumulate extra-telomeric DNA damage due to fusion-bridge-breakage cycles

3.1.1. J.
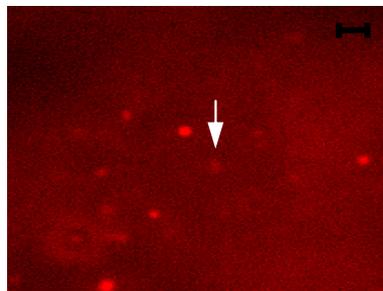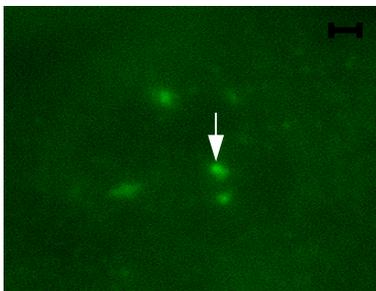
| **Telomere** | **γH2AX** | **TIF** |
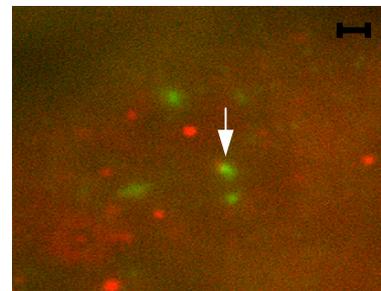

3.1.1. K.
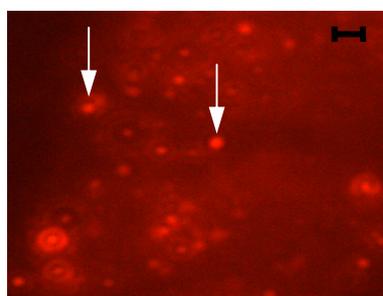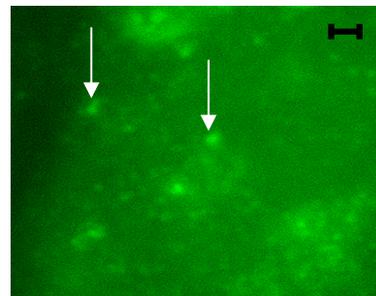
| **Telomere** | **53BP1** | **TIF** |
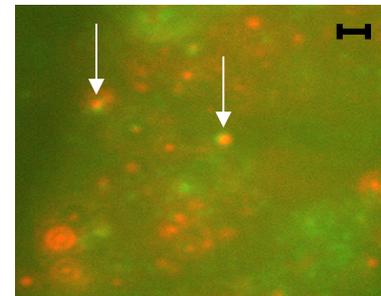
3.1.1. L.
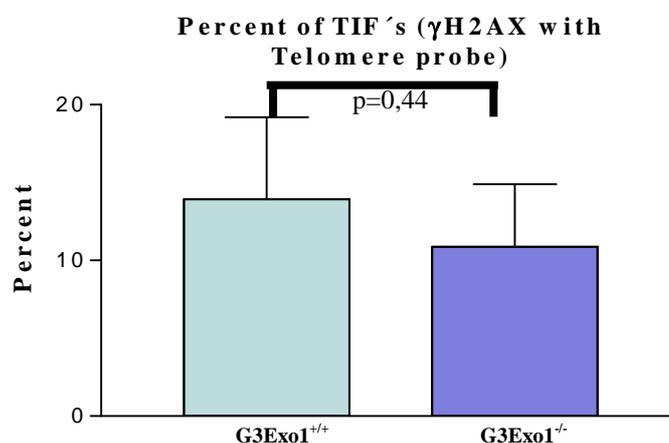
3.1.1. J. Representative photograph showing telomere signals (left), γ-H2AX–foci (middle) and co-localization of both signals (TIF, Telomere Induced Foci, right) in intestinal epithelium of 12-15 month old G3mice.**K.** Representative photograph showing telomere signals (left), 53BP1–foci (middle) and co-localization of both signals (right) in intestinal epithelium of 12-15 month old G3 mice. **L.** Histogram showing percent of TIF´s on the indicated genotypes (14% of the γH2AX-foci co-localized with telomeres).

**3.1.2. Exo1 deletion impairs the formation of ATR foci in telomere dysfunctional mice.**

Together, our results suggested that *Exo1* deletion improved organ maintenance and survival of telomere dysfunctional mice by rescuing very upstream induction of DNA damage signals. Studies in yeast have shown that EXO1 generates single stranded DNA (ssDNA) at dysfunctional telomeres, which appears to be necessary for the induction of DNA damage signals. The generation of ssDNA in response to DNA damage leads to an activation of ATR, which can thus serve as an indirect marker for ssDNA generation in response to DNA damage (Namiki and Zou, 2006; Stein et al., 1999; Zou and Elledge, 2003). To analyze whether activation of ATR was detectable in organ system affected by telomere shortening immunhistochemistry staining was carried out on mouse intestine. ATR foci were not present in *mTerc$^{+/+}$* mice. Notably, 12-15 month old G3 *mTerc$^{-/-}$, Exo1$^{+/+}$* mice showed nuclear foci of ATR in intestinal basal crypts (3.1.2.A and B), but ATR foci formation was highly dependent on *Exo1* gene status and it was not present in 12-15 month old G3 *mTerc$^{-/-}$, Exo1$^{-/-}$* mice (n=4 mice per group, p= 0.001). In agreement with our above results on organ homeostasis and cellular checkpoints, we observed a re-induction of ATR foci in nuclei of intestinal basal crypts in 24 month old G3*mTerc$^{-/-}$, Exo1$^{-/-}$* mice indicating that EXO1-independent mechanisms can activate ATR in very old double knockout mice.

Together, these results indicated that Exo1 deletion rescued organ maintenance and survival of G3*mTerc$^{-/-}$* mice by impairing the very upstream induction of DNA damage signals.

3.1.2.A.

G3Exo1+/+   **G3Exo1-/-**   **mTerc+/+Exo1+/+**
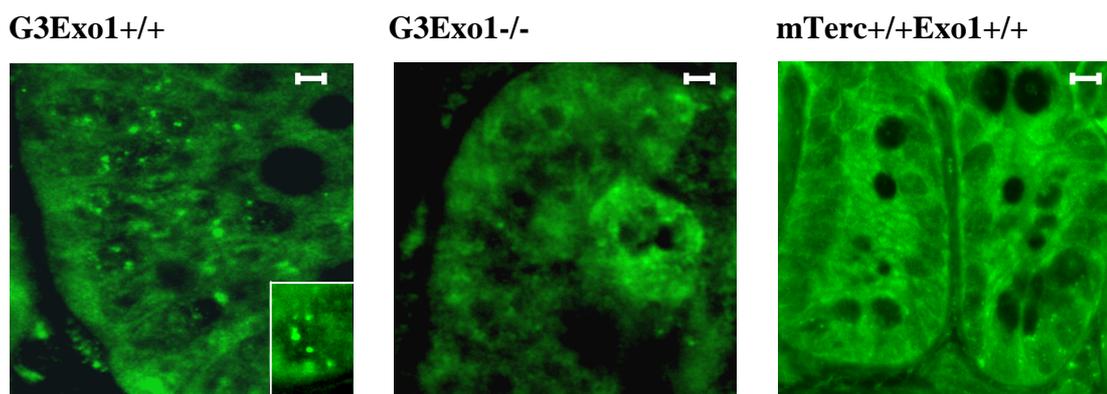
3.1.2.B.
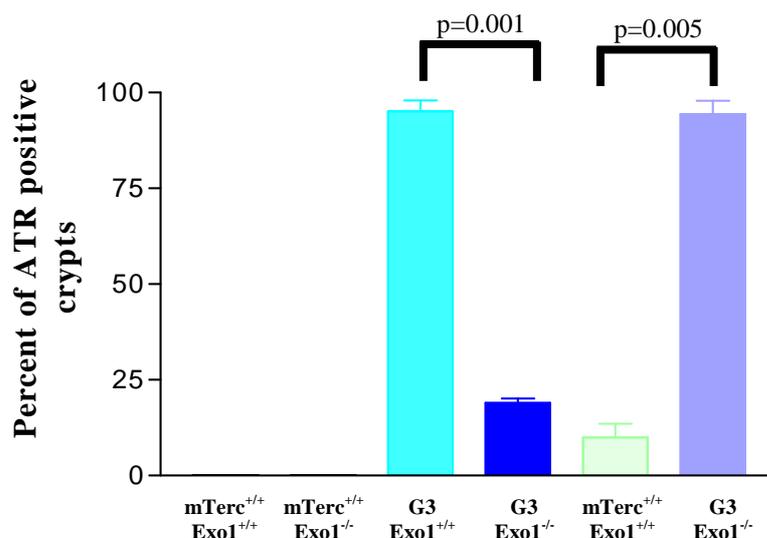
3.1.2.A. Representative photographs showing ATR-foci in nuclei of cells in basal crypts of 12-15 month old mice of the indicated genotypes (magnification bar 50 µm). **B.** Histogram showing the percentage of ATR positive basal crypts in 12-15 and 24 month old mice of the indicated genotypes (n= 4-5 mice/group).

3.1.3. *Exo1* deletion reduces cell cycle arrest and apoptosis in intestinal crypts of mice in response to γ-irradiation -

As mentioned earlier *Exo1* deletion rescued the life span and intestinal atophy due to apoptosis in G3*mTerc$^{-/-}$*. So we wanted to analyze whether the effects of *Exo1* deletion on impairment of apoptosis and cell cycle arrest were specific for telomeric DNA damage or reflected a more general role of EXO1 in response to DNA damage. We analyzed cell cycle arrest and apoptosis in basal intestinal crypts of *Exo1$^{+/+}$* and *Exo1$^{-/-}$* mice (for all irradiation studies always *mTerc$^{+/+}$* mice were used) was in response to 4Gy γ-irradiation (IR) (n= 5 mice per group, 24 hrs after IR). This analysis revealed that *Exo1* deletion significantly rescued cell cycle arrest (p=0.01) (Figure 3.1.3.A and C) and apoptosis (p= 0.03) (Figure 3.1.2.B and D) in basal intestinal crypts in response to γ-IR.
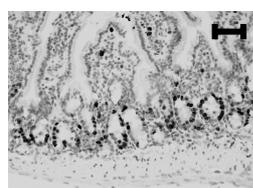
3.1.3.A.
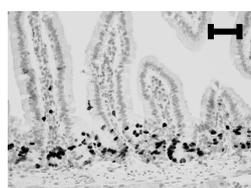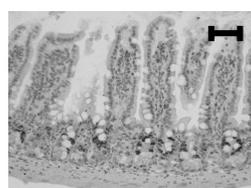
**NIRExo1+/+**   **NIRExo1-/-**   **IRExo1+/+**   **IRExo1-/-**
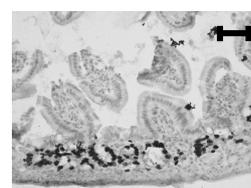
3.1.3.B.

NIRExo1+/+	NIRExo1-/-	IRExo1+/+	IRExo1-/-
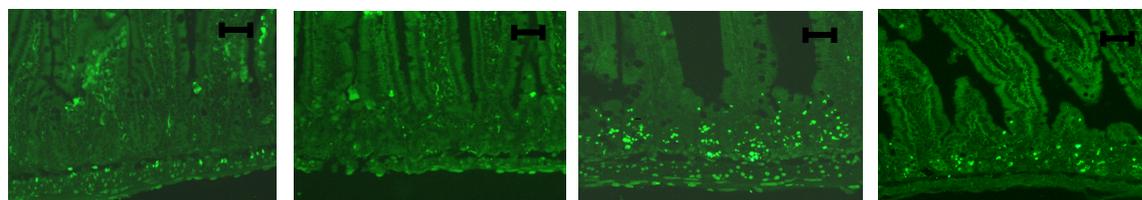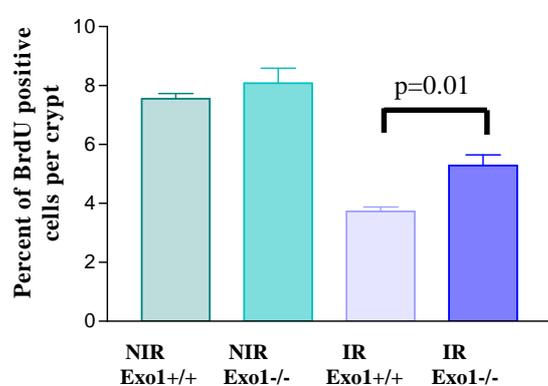
**3.1.3.C.**   **3.1.3.D.**
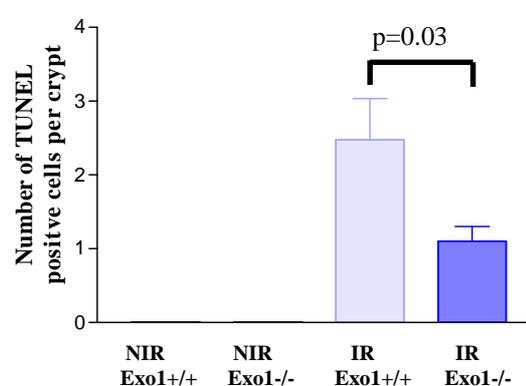
3.1.3.A. Representative photographs of BrdU-stained crypts in the small intestine of 4 month old mice: 24 hours after 4Gy γ-irradiation (IR) and non-irradiated mice (NIR) of the indicated genotypes. Magnification bars: 200 µm.. **.B.** Representative photographs of TUNEL-stained crypts in small intestine of 4 month old mice: 24 hours after 4Gy γ-irradiation (IR) and non irradiated (NIR) mice of the indicated genotypes. Magnification bars: 200 µm. **.C.** Histogram showing the percentage of BrdU-positive cells per crypt in the small intestine of 4 month old irradiated (IR) and non-irradiated (NIR) mice of the indicated genotypes (n=5 mice/group) **.D.** Histogram showing the number of TUNEL-positive cells per crypt in the small intestine of 4 month old irradiated (IR) and non irradiated (NIR) mice of the indicated genotypes (n=5 mice/group).

Similar to the results on telomere dysfunctional mice, we observed a significant reduction in the number of DNA damage foci except in γH2AX (Figure 3.1.3.E-H) levels in γ-irradiated $Exo1^{-/-}$ compared to $Exo1^{+/+}$ mice.

3.1.3.E.
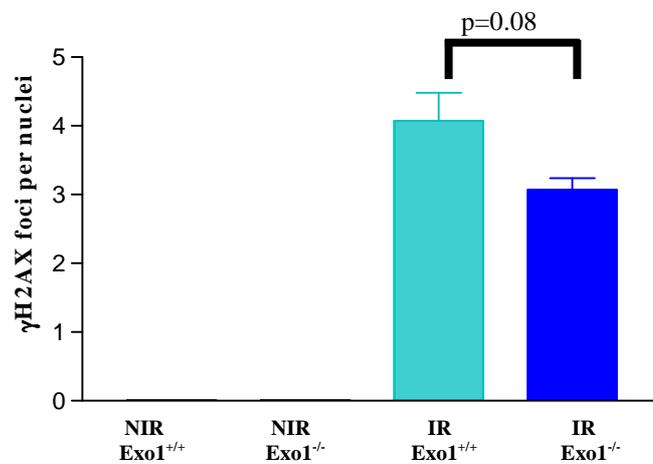

3.1.3.F.
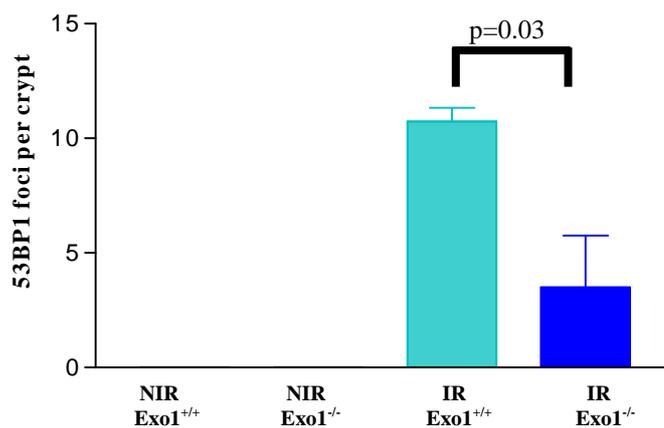
3.1.3.G.
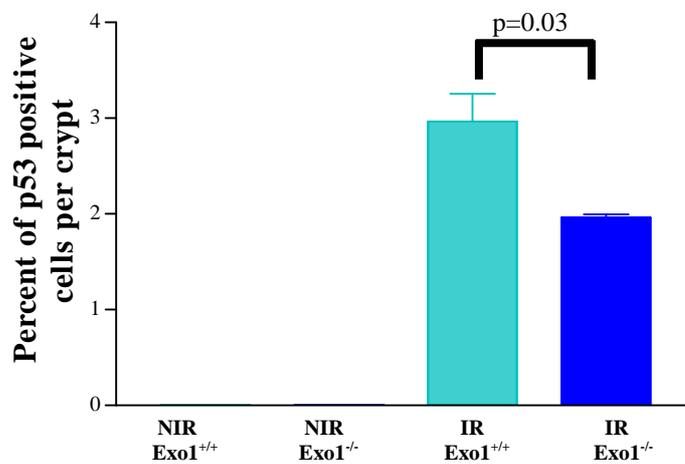
3.1.3.H.
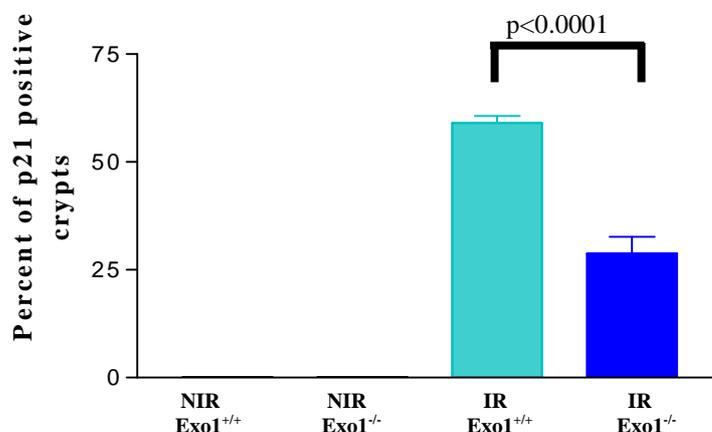
Fig. 3.1.3.E. Histogram showing the number of γ-H2AX foci per nuclei in basal crypts of 4 month old mice of the indicated genotypes (n= 5 mice/group) 4 hours after 4Gy γ-irradiation. **F.** Histogram showing the number of 53BP1 foci positive cells per basal crypts in 4 month old mice of the indicated genotypes (n= 3-5 mice/group) 2 hours after 4Gy γ-irradiation. **G.** Histogram showing the percent of p53 positive cells per basal crypts in 4 months old mice of indicated genotypes (n=3-4 mice/group) **H.** Histogram showing the percentage of p21. positive cells per intestinal basal crypts of 4 month old mice of the indicated genotypes (n=4-5 mice/group) 24 hours after 4Gy irradiation.

3.1.4. *Exo1* deletion impairs G1 cell cycle arrest in response to 15Gy irradition *in vitro* and also impairs ATR foci formation at 30 minutes after 2Gy irradiation.

The above results show *Exo1* deletion impaired DNA damage responses in mouse intestinal crypts inresponse to irradiation. To determine the exact role of EXO1 in cell cycle in response to irradiation we used mouse ear fibroblasts and irradiated them with 15Gy irradiation. 24 hours after IR (15 Gy), *Exo1*$^{+/+}$ fibroblasts showed a strong cell cycle arrest at G1 stage cycle and reduction of cells in S-phase of cell cycle, but *Exo1*$^{-/-}$ fibroblasts exhibited reduced checkpoint responses (Figure 3.1.4.A,B and C). To further characterize the role of EXO1 in response to DNA damage, we analyzed DNA damage signal induction in response to γ-IR. DNA damage signaling proteins phospho ATR, phospho CHK2-T68, pan specific CHK2, phospho p53-Ser15, pan specific p53 responses were ameliorated in irradiated *Exo1*$^{-/-}$ vs. *Exo1*$^{+/+}$ fibroblasts (Figure.3.1.4.D). The ATR foci formation was also reduced at 30 minutes after 2Gy irradiation in *Exo1*$^{-/-}$ vs. *Exo1*$^{+/+}$ fibroblasts (Figure 3.1.4.E and F).

**3.1.4.A.**


BrdU

3.1.4.B.

3.1.4.C.

3.1.4.D.

ATR

pChk2-T68

Chk2- pan specific

p53- Ser15

p53- pan specific

Actin

| **NIR**
Exo1⁺/⁺ | **NIR**
Exo1⁻/⁻ | **IR**
Exo1⁺/⁺ | **IR**
Exo1⁻/⁻ |

46

3.1.4.E.

IR Exo1+/+   IR Exo1-/-
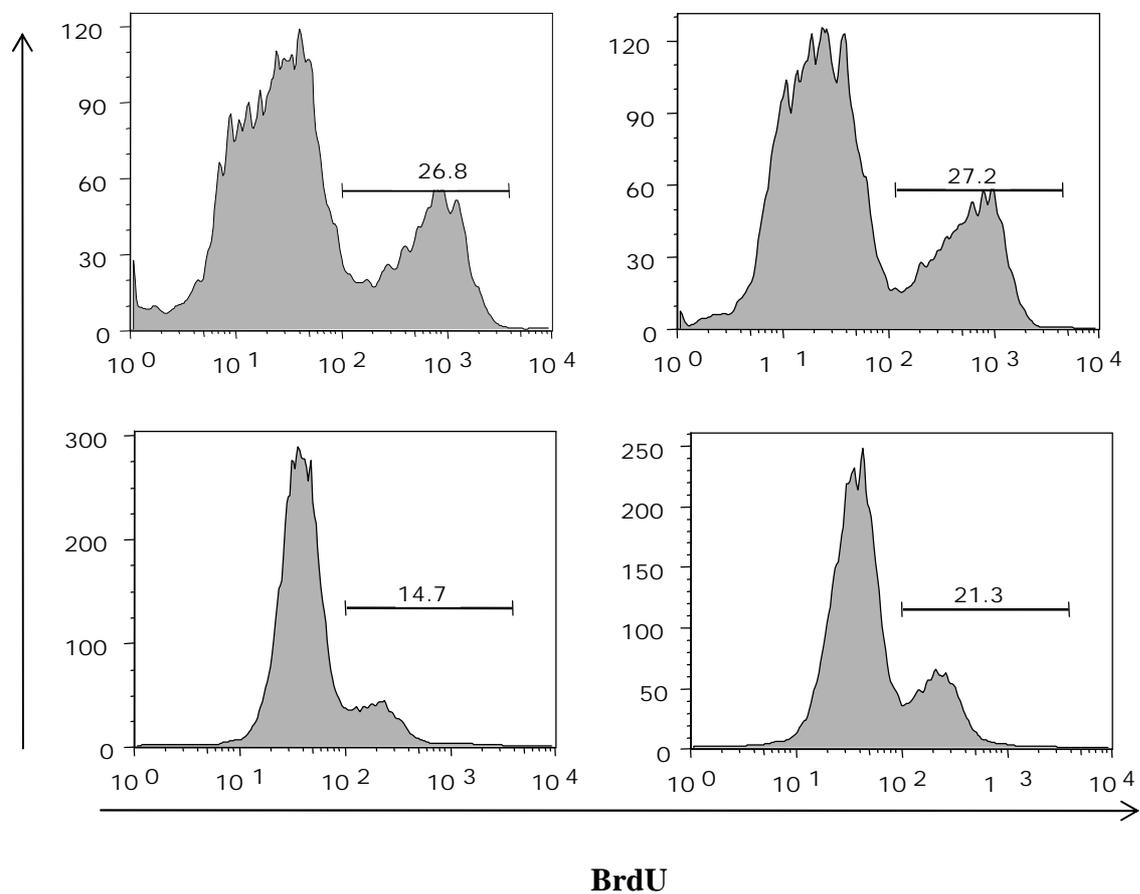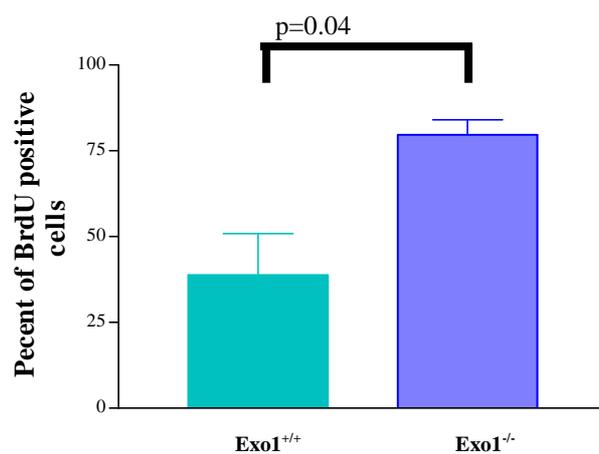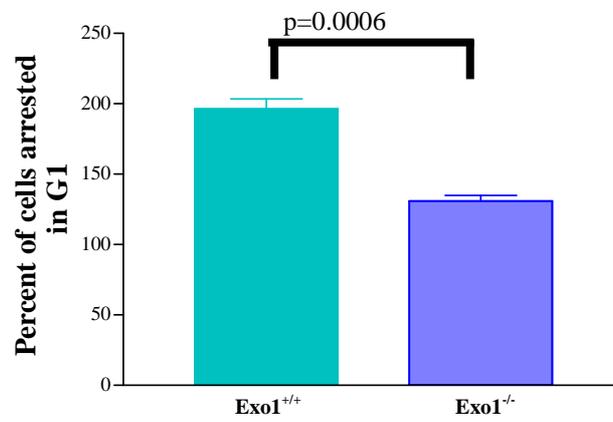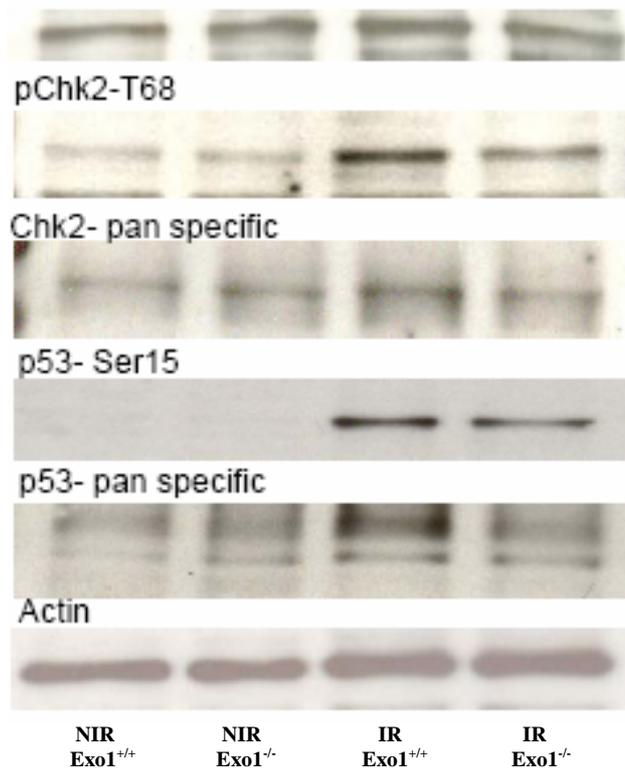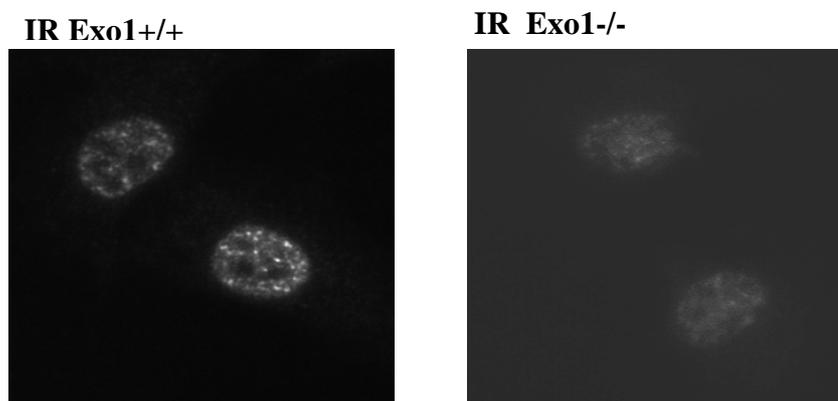
3.1.4.F.
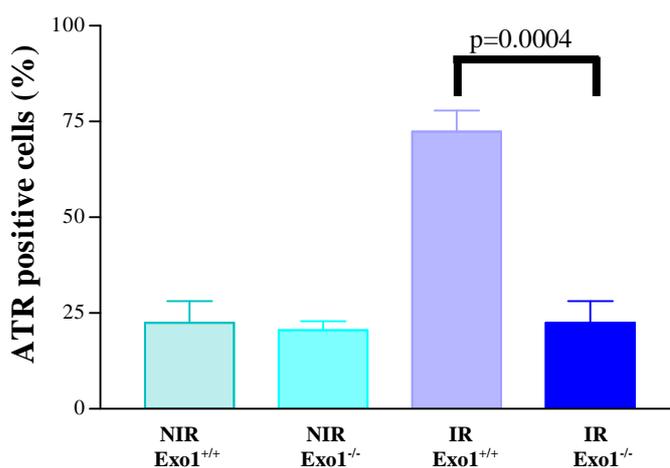
Fig. 3.1.4.A. FACS plot showing percent of BrdU positive cells at 24 hrs after 15Gy irradiation of the indicated genotypes. **B)** Histogram showing the relative reduction of BrdU positive cells in 15Gy irradiated (24 hours after IR) compared to non- irradiated cells of the indicated genotypes. **C)** Histogram showing the relative increase in cells in G1 stage of cell cycle in 15Gy irradiated (24 hours after IR) compared to non-irradiated cells of the indicated genotypes. **D)** Western blots showing expression of phosphorylated ATR (Ser345), phosphorylated CHK2 (T68), pan specific CHK2, phosphorylated p53 (Ser15) and pan specific p53 along with ß-actin as a loading control in mouse ear fibroblasts of the indicated genotypes at 24hrs after 15Gy irradiation and in non-irradiated controls(n=2-3).E) Representative pictures of ATR staining in $Exo1^{+/+}$ vs $Exo1^{-/-}$ mouse ear fibroblasts 30 minutes after 2Gy irradiation for the indicated genotypes **F)** Histogram showing ATR positive cells in $Exo1^{+/+}$ vs $Exo1^{-/-}$ mouse ear fibroblasts 30 minutes after 2Gy irradiation.

47

3.1.5. *Exo1* **deletion does not rescue lifespan of mice carrying a hypermorphic** *Rad50* **mutation.**

To further substantiate the hypothesis that Exo1 deletion rescues the very upstream induction of DNA damage signals we crossed *Exo1*^{-/-} mice with *Rad50*[s/s] mice carrying a hyperactive mutation of *Rad50* (Morales et al., 2005). The RAD50/MRE11/NBS- complex is part of the DNA damage foci at DNA breaks (Maser et al., 1997). *Rad50*[s/s] mice exhibit hypermorphic activation of DNA damage signals, which results in a severe reduction in lifespan due to bone marrow failure (Bender et al., 2002). Unlike the deletion of *Chk2* (Morales et al., 2005) the deletion of *Exo1* did not rescue lifespan of *Rad50*[s/s] mice (Figure 3.1.5) indicating that *Exo1* deletion can not rescue DNA damage signals downstream of RAD50 which clearly show that EXO1 mediates very upstream DNA damage signalling.
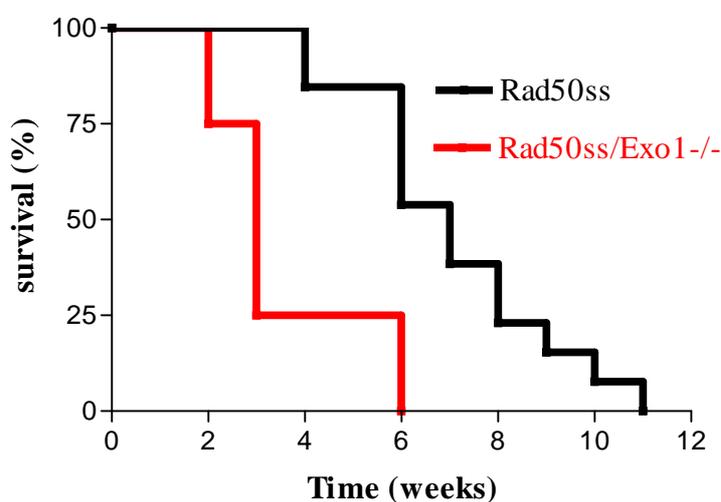

Fig.3.1.5. Survival curves are depicted for *Rad50*[s/s]*/Exo*^{+/+} (n=13) and *Rad50*[s/s]*/Exo1*^{-/-} mice (n=4) (p=0.0.0024).

3.2. 53BP1 is adown stream target of RAD50.

3.2.1. *53BP1* deletion prolongs the lifespan of mice with hyperactive *Rad50* mice.

Mice carrying a hyperactive mutation for *Rad50, Rad50$^{+/s}$* ('s' stands for mutation and '+' stands for wild type regarding the gene status of RAD50) were crossed with *53BP1$^{+/-}$* mice to get *Rad50$^{s/+}$ 53BP1$^{+/-}$* and these double heterozygotes were further crossed with each other to generat *Rad50$^{s/s}$ 53BP1$^{-/-}$* mice. These mice were in a mixed backround of 129SvEv and C57BL/6J. In agreement with previous publications, *Rad50$^{s/s}$* (n=12) mice died between the age of 6 to 12 (Figure 3.2.1.A). In contrast, none of the *Rad50$^{+/+}$53BP1$^{+/+}$* mice(n=10) and of the *Rad50$^{+/+}$53BP1$^{-/-}$* mice(n=10) died within the observation period of 12 months (Figure 3.2.1.A). Interestingly, deletion of 53BP1 prolonged the lifespan of *Rad50$^{s/s}$ 53BP1$^{+/+}$* mice. (*Rad50$^{s/s}$ 53BP1$^{-/-}$* n=11, p<0.0001).The rescue in the life span was also reflected in body weights (Figure 3.2.1.B), RBC counts (Figure 3.2.1.C) and also WBC counts (Figure 3.2.1.D) in the case of *Rad50$^{s/s}$ 53BP1$^{-/-}$*. However, the lifespan of these double mutant mice remained shortened compared to *Rad50$^{+/+}$ 53BP1$^{+/+}$* mice and the maximum lifespan of these double mutents was 6-7 months. These data suggested that 53BP1 mediates adverse effect of hyperactive RAD50 signalling. However, 53BP1 is not the only target in this pathway and other genes can apparently mediate downstream effects of hyperactive RAD50 signalling.
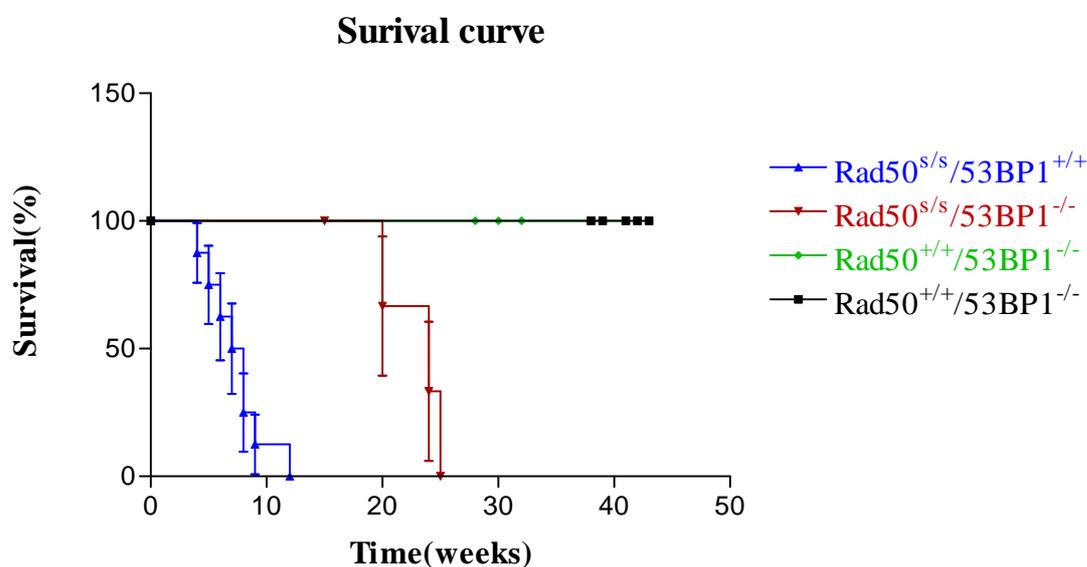
Fig.3.2.1.A. Survival curves for *Rad50$^{s/s}$/53BP1$^{+/+}$* (n=13) and *Rad50$^{s/s}$/53BP1$^{-/-}$* mice (n=11) (p<0.0.0001).

Body weights of mice at the age of 6 weeks
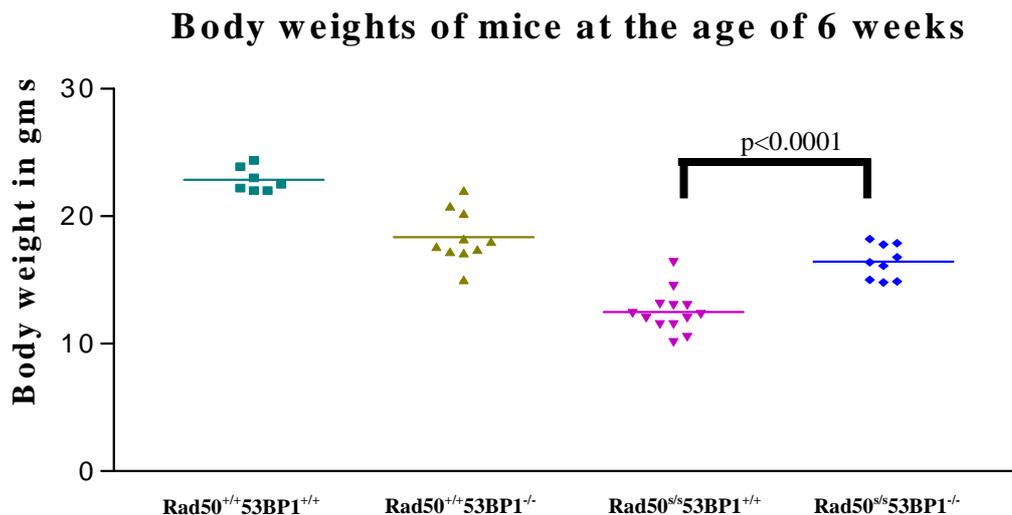
Fig.3.2.1.B. Histograph showing body weights for $Rad50^{s/s}/53BP1^{+/+}$ (n=13) and $Rad50^{s/s}/53BP1^{-/-}$ mice (n=9) (p<0.0.0001).
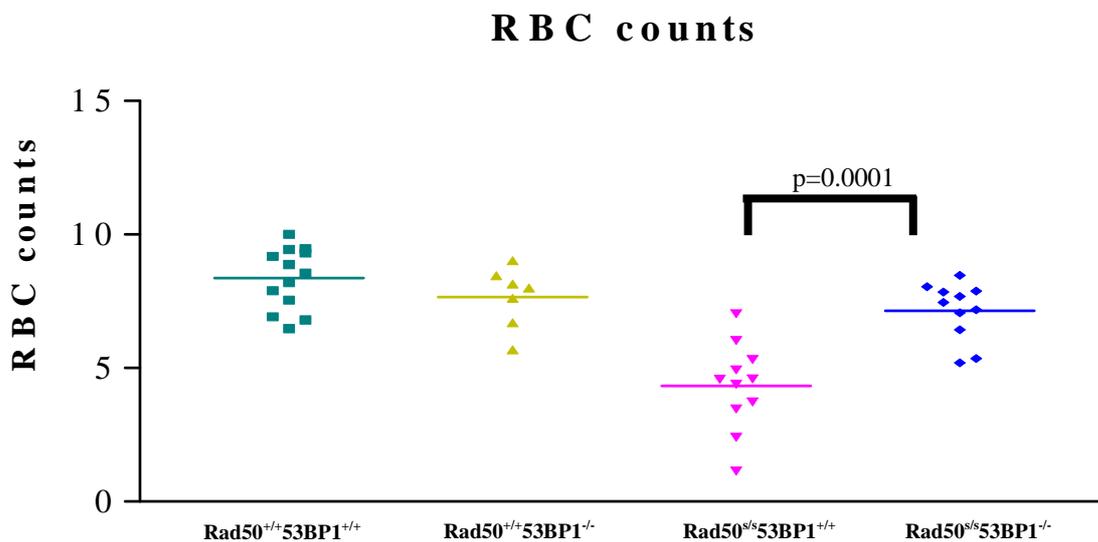
R B C   c o u n t s

Fig. 3.2.1.C. Histograph showing RBC counts for $Rad50^{s/s}/53BP1^{+/+}$ (n=11) and $Rad50^{s/s}/53BP1^{-/-}$ mice (n=11) (p=0.0001).

W B C   c o u n t s

Fig. 3.2.1.D. Histrograph showing WBC counts for *Rad50$^{s/s}$/53BP1$^{+/+}$* (n=11) and *Rad50$^{s/s}$/53BP1$^{-/-}$* mice (n=11)

3.2.2. *53BP1* deletion rescues haematopoietic failure of *Rad50$^{s/s}$* mice.

As shown in previous studies, *Rad50$^{s/s}$ 53BP1$^{+/+}$* mice have severe failure of haematopoietic compartment. The main reason for bone marrow failure is because of the activation of DNA damage check point signalling which takes the cell towards apoptosis (Bender et al., 2002). Due to apoptosis the mice suffers from anaemia and dies with in 2-3 months. In our studies, we observed that this haematopoietic failure in *Rad50$^{s/s}$/53BP1$^{+/+}$* mice was partially rescued by the deletion o*f 53BP1*. In *Rad50$^{s/s}$/53BP1$^{-/-}$* mice the number of stem cells (Lin -, Sca1+, cKit+) were 2-3 times higher than the number of LSK cells in age-matched *Rad50$^{s/s}$/53BP1$^{+/+}$* mice. However the rescue in LSK number was partial and the number of LSK cells in *Rad50$^{s/s}$/53BP1$^{-/-}$* mice remained reduced compared to *Rad50$^{+/+}$ 53BP1$^{+/+}$* mice (Figure 3.2.2.B). Similarly the number of B-lymphocytes (B220+ cells) and also the number of immature B cells (Pre B cell stage,B220+CD43-) in bone marrow was partially rescued in *Rad50$^{s/s}$/53BP1$^{-/-}$* mice compared to *Rad50$^{s/s}$ 53BP1$^{+/+}$* mice, but remained reduced compared to *Rad50$^{+/+}$ 53BP1$^{+/+}$* mice (Figure 3.2.2.C,D).

Fig 3.2.2.A. Representative FACS profiles of Lin-Sca1+ckit+ cells for the indicated genotypes
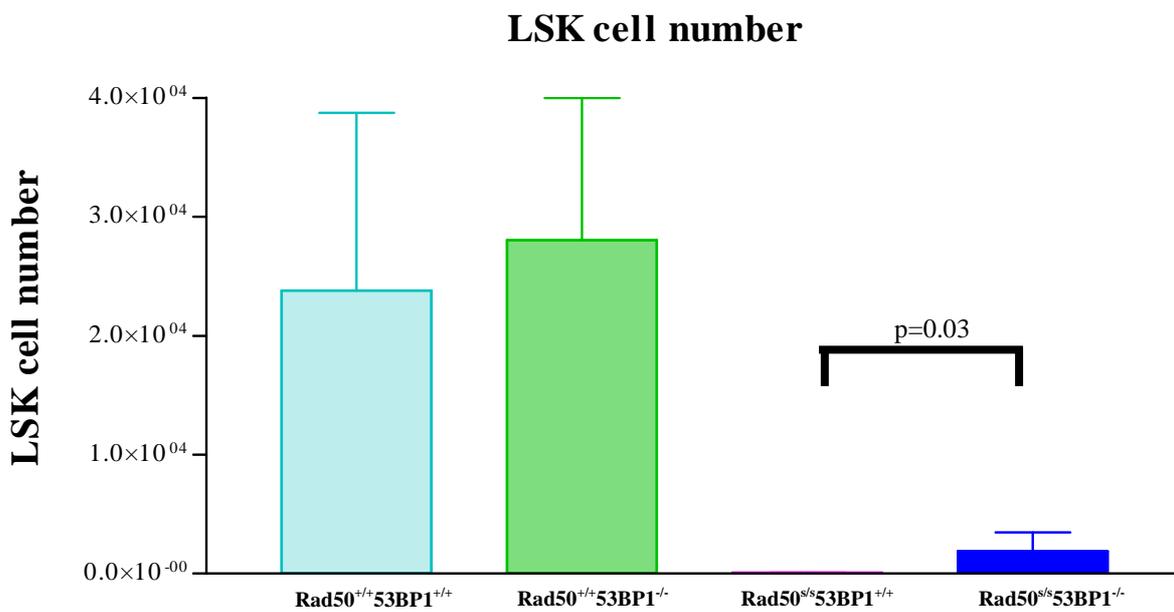
**Fig . 3.2.2.B.** Histograph showing LSK cells. *Rad50^{s/s}/53BP1^{+/+}* (n=5) and *Rad50^{s/s}/53BP1^{-/-}* mice (n=5) (p=0.03).
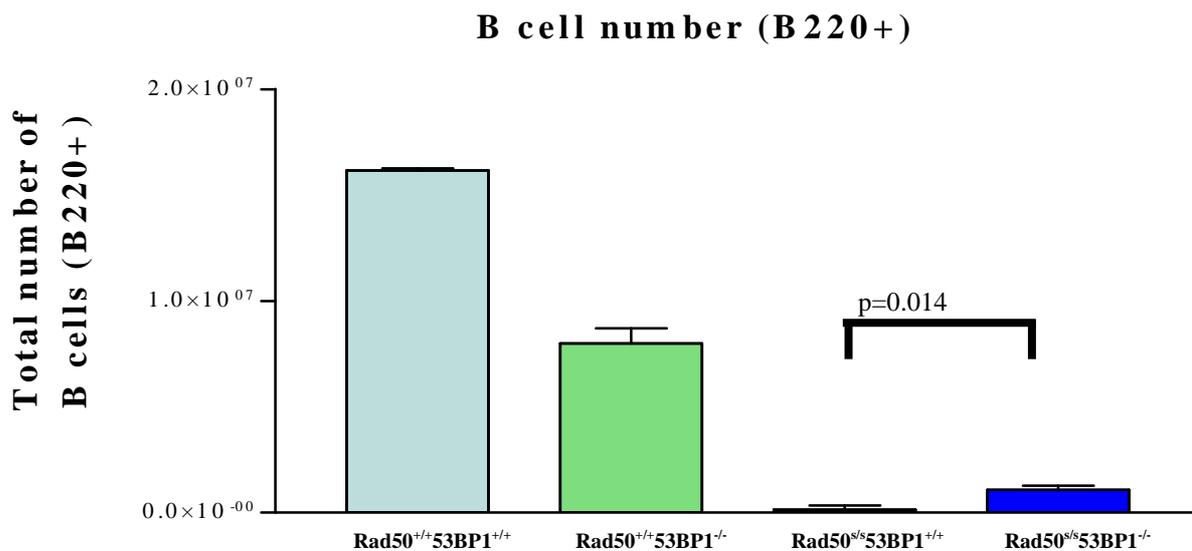
B cell number (B220+)

Fig..3.2.2..C.. Histograph showing total B cell number. *Rad50^{s/s}/53BP1^{+/+}* (n=4) and *Rad50^{s/s}/53BP1^{-/-}* mice (n=3) (p=0.001).

Number of Pre B (B220+ CD43-)cells
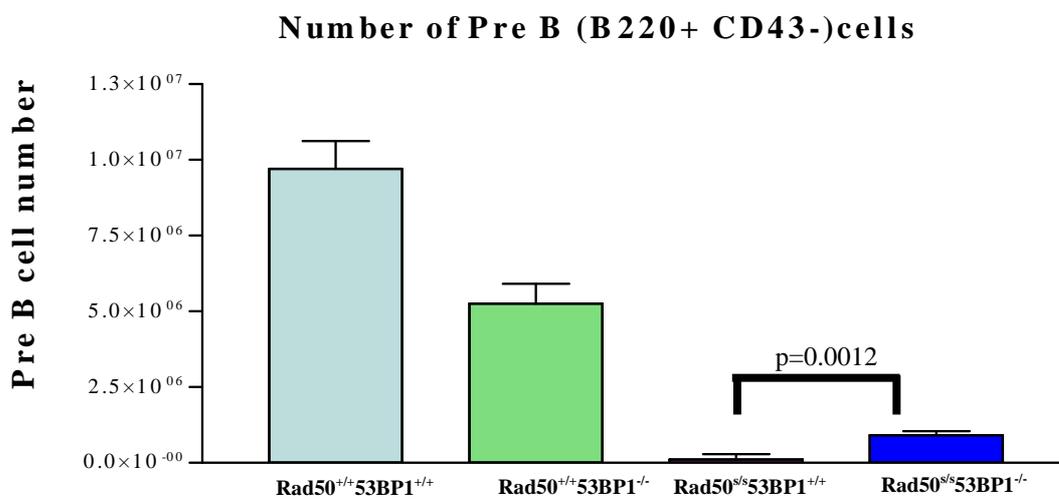

Fig. 3.2.2.D. Histograph showing Pre B cell number. *Rad50^{s/s}/53BP1^{+/+}* (n=4) and *Rad50^{s/s}/53BP1^{-/-}* mice (n=3) (p=0.0012).

3.2.3. *53BP*1 deletion reduces the rate of apoptosis due to hyper activation of RAD50 in *Rad50ss* mice.

As there was a rescue in LSK compartment and B cell compartment we check whether 53BP1 also could rescue the rate of apoptosis in B cell compartment (B220+,Ann+,7AAD-), where we observed that $Rad50^{s/s}/53BP1^{-/-}$ show reduced levels of apoptosis in the B cell compartment when compared to $Rad50^{s/s}$ mice (Figure 3.2.4).
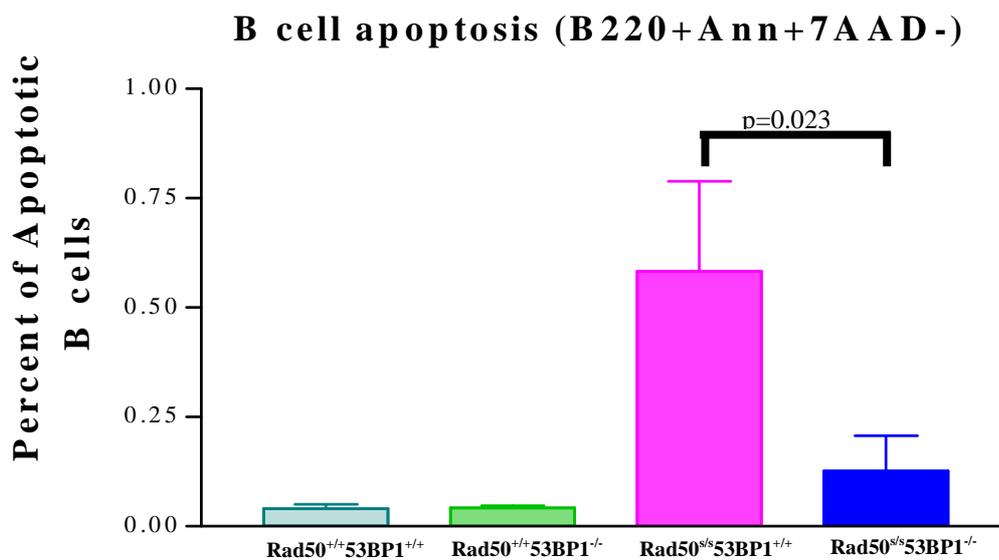
**Fig.3.2.4**. Histograph showing percent of apoptosis in B cell compartment of bone marrow. $Rad50^{s/s}/53BP1^{+/+}$ (n=4) and $Rad50^{s/s}/53BP1^{-/-}$ mice (n=3) (p=0.0012).

4. Discussion.

This study provides direct experimental evidence that EXO1 induces DNA damage responses in mammalian cells. Moreover, Exo1 deletion prevents the accumulation of DNA damage and prolongs lifespan of telomere dysfunctional mice. This study also provides *in vivo* evidence that 53BP1 is a down stream target of Rad50 and Rad50 signalling is partially dependent on 53BP1 in response to dsDNA damage.

4.1. *Exo1* Deletion Impairs the Induction of DNA Damage Signals

The current study shows that Exo1 deletion impairs the induction of checkpoint responses and confers resistance of mammalian cells and organs to γ-IR and telomere dysfunction. The study points to the formation of ssDNA as one mechanism by which EXO1 amplifies the generation of DNA damage signals at DNA breaks. Previous studies on yeast have shown that the generation of ssDNA is required for DNA damage signal induction (Garvik et al., 1995; Lee et al., 1998b; Lydall and Weinert, 1995; Zou and Elledge, 2003). Similar mechanisms exist in mammalian cells (Zou and Elledge, 2003). However, the molecular mechanisms leading to the formation of ssDNA in response to DNA damage are not completely understood. In yeast, EXO1 has been shown to induce ssDNA in response to telomere dysfunction (Maringele and Lydall, 2002). Our study provides, to our knowledge, the first evidence that the nuclease domain of EXO1 participates in the formation of ssDNA and ATR activation at DNA double-strand breaks and in response to telomere dysfunction in mammalian cells. This mechanism likely contributes to aggravate phenotypes of telomere dysfunction in mTerc$^{-/-}$ mice.

4.2. *Exo1* Deletion Impairs the Accumulation of DNA Damage in Telomere-dysfunctional Mice.

Although EXO1 does not prevent γH2AX foci formation in response to γ-IR and laser treatment, Exo1 deletion markedly reduced the accumulation of γH2AX foci in vivo in mTerc$^{-/-}$ mice. These data indicate that dysfunctional telomeres induce EXO1-dependent processes that lead to an accumulation of further DNA damage. Cells having undergone replicative senescence due to telomere shortening display numerous γH2AX foci throughout the genome that do not colocalize with telomeric regions (Sedelnikova et al., 2004). It is possible that *Exo1* deletion reduces the secondary formation of DNA damage in response to telomere dysfunction by inhibiting chromosomal fusions and fusion-bridge-breakage cycles that create

extratelomeric DNA damage in telomere-dysfunctional mice. In agreement with this hypothesis, *Exo1* deletion reduces the number of anaphase bridges in telomere-dysfunctional mice (Schaetzlein et al., 2007). Other, less obvious mechanisms might be involved. It has been shown that telomere dysfunction increases intracellular ROS levels in senescent cells (Passos et al., 2007). Although the exact mechanisms are not understood, it is possible that deletion of *Exo1* also reduces the accumulation of ROS and thereby the accumulation of DNA damage in senescent cells. Therefore, it is conceivable that EXO1 has different, additive effects on DNA damage accumulation and DNA damage signal induction in telomere dysfunctional mice. Its role in DNA break processing could directly contribute to the induction of DNA damage signals. In addition, EXO1 could increase the generation of extratelomeric DNA damage in the context of chronic telomere dysfunction. An accumulation of extratelomeric DNA damage has been associated with organismal ageing (Sedelnikova et al., 2004). Based on our study, it is intriguing to speculate that EXO1-dependent processes contribute to this phenomenon.

4.3. 53BP1-a down stream target of RAD50.

As we know that Rad50 complex plays a crucial role in the amplification of DNA damage signalling upstream to ATM (Lee and Paull, 2004) after DNA damage signal initiation It is also known that 53BP1 is down stream to γH2AX(Ward et al., 2003a). But γH2AX is known to be as a downstream target of ATM. Recent experiments prove that 53BP1 functions upstream to ATM in the DNA damage signalling pathway (Zgheib et al., 2005). Now, as ATM is proved to be a downstream target of Rad50 (Lee and Paull, 2004) it is certainly important to know the exact position of 53BP1 in this DNA damage signalling pathway. There fore we used Rad50$^{s/s}$ mouse model carrying hyperactivation of DNA damage signalling pathway as an in vivo model to check whether 53BP1 is upstream or down stream to Rad50. Removal of 53BP1 from the Rad50$^{s/s}$ mice rescued the heamatopiotic failure of hypermorphic mice and there by increase the survial of Rad50$^{s/s}$ mice. This gives the in vivo experimental evidence that 53BP1 is a down stream target of Rad50 in the DNA damage signalling.

Reference List

Abraham,R.T. (2001). Cell cycle checkpoint signaling through the ATM and ATR kinases. Genes Dev. *15*, 2177-2196.

Allsopp,R.C., Chang,E., Kashefi-Aazam,M., Rogaev,E.I., Piatyszek,M.A., Shay,J.W., and Harley,C.B. (1995). Telomere shortening is associated with cell division in vitro and in vivo. Exp. Cell Res. *220*, 194-200.

Allsopp,R.C. and Harley,C.B. (1995). Evidence for a critical telomere length in senescent human fibroblasts. Exp. Cell Res. *219*, 130-136.

Artandi,S.E., Chang,S., Lee,S.L., Alson,S., Gottlieb,G.J., Chin,L., and DePinho,R.A. (2000). Telomere dysfunction promotes non-reciprocal translocations and epithelial cancers in mice. Nature *406*, 641-645.

Autexier,C. and Lue,N.F. (2006). The Structure and Function of Telomerase Reverse Transcriptase. Annu. Rev. Biochem.

Aviv,A., Levy,D., and Mangel,M. (2003). Growth, telomere dynamics and successful and unsuccessful human aging. Mech. Ageing Dev. *124*, 829-837.

Bakkenist,C.J. and Kastan,M.B. (2003). DNA damage activates ATM through intermolecular autophosphorylation and dimer dissociation. Nature *421*, 499-506.

Banin,S., Moyal,L., Shieh,S., Taya,Y., Anderson,C.W., Chessa,L., Smorodinsky,N.I., Prives,C., Reiss,Y., Shiloh,Y., and Ziv,Y. (1998). Enhanced phosphorylation of p53 by ATM in response to DNA damage. Science *281*, 1674-1677.

Barlow,C., Hirotsune,S., Paylor,R., Liyanage,M., Eckhaus,M., Collins,F., Shiloh,Y., Crawley,J.N., Ried,T., Tagle,D., and Wynshaw-Boris,A. (1996). Atm-deficient mice: a paradigm of ataxia telangiectasia. Cell *86*, 159-171.

Bender,C.F., Sikes,M.L., Sullivan,R., Huye,L.E., Le Beau,M.M., Roth,D.B., Mirzoeva,O.K., Oltz,E.M., and Petrini,J.H. (2002). Cancer predisposition and hematopoietic failure in Rad50(S/S) mice. Genes Dev. *16*, 2237-2251.

Blackburn,E.H. (1997). The telomere and telomerase: nucleic acid-protein complexes acting in a telomere homeostasis system. A review. Biochemistry (Mosc.) *62*, 1196-1201.

Blasco,M.A., Lee,H.W., Hande,M.P., Samper,E., Lansdorp,P.M., DePinho,R.A., and Greider,C.W. (1997). Telomere shortening and tumor formation by mouse cells lacking telomerase RNA. Cell *91*, 25-34.

Brown,A.L., Lee,C.H., Schwarz,J.K., Mitiku,N., Piwnica-Worms,H., and Chung,J.H. (1999). A human Cds1-related kinase that functions downstream of ATM protein in the cellular response to DNA damage. Proc. Natl. Acad. Sci. U. S. A *96*, 3745-3750.

Brown,E.J. and Baltimore,D. (2000). ATR disruption leads to chromosomal fragmentation and early embryonic lethality. Genes and Development *14*, 397-402.

Brown,J.P., Wei,W., and Sedivy,J.M. (1997). Bypass of Senescence After Disruption of p21CIP1/WAF1 Gene in Normal Diploid Human Fibroblasts. Science *277*, 831-834.

Buscemi,G., Savio,C., Zannini,L., Micciche,F., Masnada,D., Nakanishi,M., Tauchi,H., Komatsu,K., Mizutani,S., Khanna,K., Chen,P., Concannon,P., Chessa,L., and Delia,D. (2001). Chk2 activation dependence on Nbs1 after DNA damage. Mol. Cell Biol. *21*, 5214-5222.

Celeste,A., Fernandez-Capetillo,O., Kruhlak,M.J., Pilch,D.R., Staudt,D.W., Lee,A., Bonner,R.F., Bonner,W.M., and Nussenzweig,A. (2003). Histone H2AX phosphorylation is dispensable for the initial recognition of DNA breaks. Nat. Cell Biol. *5*, 675-679.

Chehab,N.H., Malikzay,A., Stavridi,E.S., and Halazonetis,T.D. (1999). Phosphorylation of Ser-20 mediates stabilization of human p53 in response to DNA damage. Proc. Natl. Acad. Sci. U. S. A *96*, 13777-13782.

Chin,L., Artandi,S.E., Shen,Q., Tam,A., Lee,S.L., Gottlieb,G.J., Greider,C.W., and DePinho,R.A. (1999). p53 deficiency rescues the adverse effects of telomere loss and cooperates with telomere dysfunction to accelerate carcinogenesis. Cell *97*, 527-538.

Chiu,C.P., Dragowska,W., Kim,N.W., Vaziri,H., Yui,J., Thomas,T.E., Harley,C.B., and Lansdorp,P.M. (1996). Differential expression of telomerase activity in hematopoietic progenitors from adult human bone marrow. Stem Cells *14*, 239-248.

Choudhury,A.R., Ju,Z., Djojosubroto,M.W., Schienke,A., Lechel,A., Schaetzlein,S., Jiang,H., Stepczynska,A., Wang,C., Buer,J., Lee,H.W., Von Zglinicki,T., Ganser,A., Schirmacher,P., Nakauchi,H., and Rudolph,K.L. (2007). Cdkn1a deletion improves stem cell function and lifespan of mice with dysfunctional telomeres without accelerating cancer formation. Nat. Genet. *39*, 99-105.

d'Adda,d.F., Reaper,P.M., Clay-Farrace,L., Fiegler,H., Carr,P., Von Zglinicki,T., Saretzki,G., Carter,N.P., and Jackson,S.P. (2003). A DNA damage checkpoint response in telomere-initiated senescence. Nature *426*, 194-198.

de Laat,W.L., Jaspers,N.G., and Hoeijmakers,J.H. (1999). Molecular mechanism of nucleotide excision repair. Genes Dev. *13*, 768-785.

de Lange,T. (2005). Shelterin: the protein complex that shapes and safeguards human telomeres. Genes Dev. *19*, 2100-2110.

el Deiry,W.S., Tokino,T., Velculescu,V.E., Levy,D.B., Parsons,R., Trent,J.M., Lin,D., Mercer,W.E., Kinzler,K.W., and Vogelstein,B. (1993). WAF1, a potential mediator of p53 tumor suppression. Cell *75*, 817-825.

Featherstone, C. and Jackson, S. P. DNA double-strand break repair. Curr.Biol. 9[20], R759-R761. 21-10-1999.
Ref Type: Journal (Full)

Garvik,B., Carson,M., and Hartwell,L. (1995). Single-stranded DNA arising at telomeres in cdc13 mutants may constitute a specific signal for the RAD9 checkpoint. Mol. Cell Biol. *15*, 6128-6138.

Giaccia,A.J. and Kastan,M.B. (1998). The complexity of p53 modulation: emerging patterns from divergent signals. Genes Dev. *12*, 2973-2983.

Gire,V., Roux,P., Wynford-Thomas,D., Brondello,J.M., and Dulic,V. (2004). DNA damage checkpoint kinase Chk2 triggers replicative senescence. EMBO J. *23*, 2554-2563.

Greenberg,R.A., Allsopp,R.C., Chin,L., Morin,G.B., and DePinho,R.A. (1998). Expression of mouse telomerase reverse transcriptase during development, differentiation and proliferation. Oncogene *16*, 1723-1730.

Greider,C.W. (1991). Telomeres. Curr. Opin. Cell Biol. *3*, 444-451.

Greider,C.W. and Blackburn,E.H. (1989). A telomeric sequence in the RNA of Tetrahymena telomerase required for telomere repeat synthesis. Nature *337*, 331-337.

Hackett,J.A. and Greider,C.W. (2003). End resection initiates genomic instability in the absence of telomerase. Mol. Cell Biol. *23*, 8450-8461.

Harper,J.W., Adami,G.R., Wei,N., Keyomarsi,K., and Elledge,S.J. (1993). The p21 Cdk-interacting protein Cip1 is a potent inhibitor of G1 cyclin-dependent kinases. Cell *75*, 805-816.

Hayflick,L. (1965). THE LIMITED IN VITRO LIFETIME OF HUMAN DIPLOID CELL STRAINS. Exp. Cell Res. *37*, 614-636.

Hemann,M.T. and Greider,C.W. (2000). Wild-derived inbred mouse strains have short telomeres. Nucleic Acids Res. *28*, 4474-4478.

Herbig,U., Jobling,W.A., Chen,B.P., Chen,D.J., and Sedivy,J.M. (2004). Telomere shortening triggers senescence of human cells through a pathway involving ATM, p53, and p21(CIP1), but not p16(INK4a). Mol. Cell *14*, 501-513.

Hoffmann,I., Draetta,G., and Karsenti,E. (1994). Activation of the phosphatase activity of human cdc25A by a cdk2-cyclin E dependent phosphorylation at the G1/S transition. EMBO J. *13*, 4302-4310.

Hubscher,U., Maga,G., and Spadari,S. (2002). Eukaryotic DNA polymerases. Annu. Rev. Biochem. *71*, 133-163.

Jazayeri,A., Falck,J., Lukas,C., Bartek,J., Smith,G.C., Lukas,J., and Jackson,S.P. (2006). ATM- and cell cycle-dependent regulation of ATR in response to DNA double-strand breaks. Nat. Cell Biol. *8*, 37-45.

Kondo,T., Wakayama,T., Naiki,T., Matsumoto,K., and Sugimoto,K. (2001). Recruitment of Mec1 and Ddc1 checkpoint proteins to double-strand breaks through distinct mechanisms. Science *294*, 867-870.

Lee,H.W., Blasco,M.A., Gottlieb,G.J., Horner,J.W., Greider,C.W., and DePinho,R.A. (1998a). Essential role of mouse telomerase in highly proliferative organs. Nature *392*, 569-574.

Lee,H.W., Blasco,M.A., Gottlieb,G.J., Horner,J.W., Greider,C.W., and DePinho,R.A. (1998b). Essential role of mouse telomerase in highly proliferative organs. Nature *392*, 569-574.

Lee,J.H. and Paull,T.T. (2004). Direct activation of the ATM protein kinase by the Mre11/Rad50/Nbs1 complex. Science *304*, 93-96.

Liu,Y., Kha,H., Ungrin,M., Robinson,M.O., and Harrington,L. (2002). Preferential maintenance of critically short telomeres in mammalian cells heterozygous for mTert. Proc. Natl. Acad. Sci. U. S. A *99*, 3597-3602.

Lowndes,N.F. and Murguia,J.R. (2000). Sensing and responding to DNA damage. Curr. Opin. Genet. Dev. *10*, 17-25.

Lundblad,V. (1997). The end replication problem: more than one solution. Nat. Med. *3*, 1198-1199.

Lydall,D. and Weinert,T. (1995). Yeast checkpoint genes in DNA damage processing: implications for repair and arrest. Science *270*, 1488-1491.

Maiti,B., Li,J., de Bruin,A., Gordon,F., Timmers,C., Opavsky,R., Patil,K., Tuttle,J., Cleghorn,W., and Leone,G. (2005). Cloning and characterization of mouse E2F8, a novel mammalian E2F family member capable of blocking cellular proliferation. J. Biol. Chem. *280*, 18211-18220.

Maringele,L. and Lydall,D. (2004). EXO1 plays a role in generating type I and type II survivors in budding yeast. Genetics *166*, 1641-1649.

Maringele,L. and Lydall,D. (2002). EXO1-dependent single-stranded DNA at telomeres activates subsets of DNA damage and spindle checkpoint pathways in budding yeast yku70Delta mutants. Genes and Development *16*, 1919-1933.

Melchionna,R., Chen,X.B., Blasina,A., and McGowan,C.H. (2000). Threonine 68 is required for radiation-induced phosphorylation and activation of Cds1. Nat. Cell Biol. *2*, 762-765.

Melo,J.A., Cohen,J., and Toczyski,D.P. (2001). Two checkpoint complexes are independently recruited to sites of DNA damage in vivo. Genes Dev. *15*, 2809-2821.

Meyerson,M., Counter,C.M., Eaton,E.N., Ellisen,L.W., Steiner,P., Caddle,S.D., Ziaugra,L., Beijersbergen,R.L., Davidoff,M.J., Liu,Q., Bacchetti,S., Haber,D.A., and Weinberg,R.A. (1997). hEST2, the putative human telomerase catalytic subunit gene, is up-regulated in tumor cells and during immortalization. Cell *90*, 785-795.

Morales,M., Theunissen,J.W., Kim,C.F., Kitagawa,R., Kastan,M.B., and Petrini,J.H. (2005). The Rad50S allele promotes ATM-dependent DNA damage responses and suppresses ATM deficiency: implications for the Mre11 complex as a DNA damage sensor. Genes Dev. *19*, 3043-3054.

Niida,H. and Nakanishi,M. (2006). DNA damage checkpoints in mammals. Mutagenesis *21*, 3-9.

Nyberg,K.A., Michelson,R.J., Putnam,C.W., and Weinert,T.A. (2002). Toward maintaining the genome: DNA damage and replication checkpoints. Annu. Rev. Genet. *36*, 617-656.

Passos,J.F., Saretzki,G., Ahmed,S., Nelson,G., Richter,T., Peters,H., Wappler,I., Birket,M.J., Harold,G., Schaeuble,K., Birch-Machin,M.A., Kirkwood,T.B., and Von Zglinicki,T. (2007). Mitochondrial dysfunction accounts for the stochastic heterogeneity in telomere-dependent senescence. PLoS. Biol. *5*, e110.

Paull,T.T., Rogakou,E.P., Yamazaki,V., Kirchgessner,C.U., Gellert,M., and Bonner,W.M. (2000). A critical role for histone H2AX in recruitment of repair factors to nuclear foci after DNA damage. Curr. Biol. *10*, 886-895.

Qi,L., Strong,M.A., Karim,B.O., Armanios,M., Huso,D.L., and Greider,C.W. (2003). Short telomeres and ataxia-telangiectasia mutated deficiency cooperatively increase telomere dysfunction and suppress tumorigenesis. Cancer Res. *63*, 8188-8196.

Rogakou,E.P., Pilch,D.R., Orr,A.H., Ivanova,V.S., and Bonner,W.M. (1998). DNA Double-stranded Breaks Induce Histone H2AX Phosphorylation on Serine 139. J. Biol. Chem. *273*, 5858-5868.

Rudolph,K.L., Chang,S., Lee,H.W., Blasco,M., Gottlieb,G.J., Greider,C., and DePinho,R.A. (1999). Longevity, stress response, and cancer in aging telomerase-deficient mice. Cell *96*, 701-712.

Schaetzlein,S., Kodandaramireddy,N.R., Ju,Z., Lechel,A., Stepczynska,A., Lilli,D.R., Clark,A.B., Rudolph,C., Wei,K., Schlegelberger,B., Schirmacher,P., Kunkel,T.A., Greenberg,R.A., Edelmann,W., and Rudolph,K.L. (2007). Exonuclease-1 deletion impairs DNA damage signaling and prolongs lifespan of telomere-dysfunctional mice. Cell *130*, 863-877.

Sedelnikova,O.A., Horikawa,I., Zimonjic,D.B., Popescu,N.C., Bonner,W.M., and Barrett,J.C. (2004). Senescing human cells and ageing mice accumulate DNA lesions with unrepairable double-strand breaks. Nat. Cell Biol. *6*, 168-170.

Shay,J.W. (1999). At the end of the millennium, a view of the end. Nat. Genet. *23*, 382-383.

Shay,J.W. and Wright,W.E. (2000). Implications of mapping the human telomerase gene (hTERT) as the most distal gene on chromosome 5p. Neoplasia. *2*, 195-196.

Shieh,S.Y., Ikeda,M., Taya,Y., and Prives,C. (1997). DNA damage-induced phosphorylation of p53 alleviates inhibition by MDM2. Cell *91*, 325-334.

Shiloh,Y. (1997). Ataxia-telangiectasia and the Nijmegen breakage syndrome: related disorders but genes apart. Annu. Rev. Genet. *31*, 635-662.

Sluss,H.K., Armata,H., Gallant,J., and Jones,S.N. (2004). Phosphorylation of serine 18 regulates distinct p53 functions in mice. Mol. Cell Biol. *24*, 976-984.

Takai,H., Naka,K., Okada,Y., Watanabe,M., Harada,N., Saito,S., Anderson,C.W., Appella,E., Nakanishi,M., Suzuki,H., Nagashima,K., Sawa,H., Ikeda,K., and Motoyama,N. (2002). Chk2-deficient mice exhibit radioresistance and defective p53-mediated transcription. EMBO J. *21*, 5195-5205.

Verdun,R.E., Crabbe,L., Haggblom,C., and Karlseder,J. (2005). Functional human telomeres are recognized as DNA damage in G2 of the cell cycle. Mol. Cell *20*, 551-561.

von Zglinicki,T., Burkle,A., and Kirkwood,T.B.L. (2001). Stress, DNA damage and ageing -- an integrative approach. Experimental Gerontology *36*, 1049-1062.

Wang,S. and Zhu,J. (2003). Evidence for a relief of repression mechanism for activation of the human telomerase reverse transcriptase promoter. J. Biol. Chem. *278*, 18842-18850.

Ward,I.M., Minn,K., van Deursen,J., and Chen,J. (2003). p53 Binding protein 53BP1 is required for DNA damage responses and tumor suppression in mice. Mol. Cell Biol. *23*, 2556-2563.

Wei,K., Clark,A.B., Wong,E., Kane,M.F., Mazur,D.J., Parris,T., Kolas,N.K., Russell,R., Hou,H., Jr., Kneitz,B., Yang,G., Kunkel,T.A., Kolodner,R.D., Cohen,P.E., and Edelmann,W. (2003). Inactivation of Exonuclease 1 in mice results in DNA mismatch repair defects, increased cancer susceptibility, and male and female sterility. Genes Dev. *17*, 603-614.

Wright,W.E., Piatyszek,M.A., Rainey,W.E., Byrd,W., and Shay,J.W. (1996). Telomerase activity in human germline and embryonic tissues and cells. Dev. Genet. *18*, 173-179.

Wright,W.E. and Shay,J.W. (1992). The two-stage mechanism controlling cellular senescence and immortalization. Exp. Gerontol. *27*, 383-389.

Zhou,B.B. and Elledge,S.J. (2000). The DNA damage response: putting checkpoints in perspective. Nature *408*, 433-439.

Zhu,X.D., Kuster,B., Mann,M., Petrini,J.H., and de Lange,T. (2000). Cell-cycle-regulated association of RAD50/MRE11/NBS1 with TRF2 and human telomeres. Nat. Genet. *25*, 347-352.

Zou,L. and Elledge,S.J. (2003). Sensing DNA damage through ATRIP recognition of RPA-ssDNA complexes. Science *300*, 1542-1548.

Curriculum Vitae

Nalapareddy Kodandaramireddy   **E-mail: kodandaramireddy_n@yahoo.com**

Name	N. Kodandaramireddy
Date of Birth	05-11-1977
Place of Birth	Lingalapuram Village, Andhrapradesh, INDIA
Nationality	INDIAN
Sex	Male
Marital status	Married
Father´s Name	N.Ramachandrareddy
Mother´s Name	N.Nagamma
Extracurricular activities	Martial arts-Tae kwon do
Present Address	N.Kodandaramireddy, Haus G, Room 704, Helstorfer Str-2, 30625, Hannover, Germany.

Education

SSC-10th standard	Board of Secondary Education, India.1992-1993
Intermediate	Board of Intermediate Education, India.1993 -1995
Bachelor of Science (B.Sc)	S.V.University, Tirupathi, India. 1997-2000
Master of Science (M.Sc)	S.V.University, Tirupati, India. 2000-2002
Doctoral Research	Department of Gastroenterology, Hepatology & Endocrinology, Hannover Medical School, Hannover, Germany, from June-2004
Awards & Achievements	1. Best Student Award during Bachelor´s degree study 2. NCCS (National Centre for Cell Science,Pune,India) - Junior Research Fellowship, June 2002 3. Qualified as Project Research Fellow at MKU (Madurai Kamraj University), Madurai, India, Feb 2004.

Publications

Schaetzlein,S*., **Kodandaramireddy,N.R***., Ju,Z., Lechel,A., Stepczynska,A., Lilli,D.R., Clark,A.B., Rudolph,C., Wei,K., Schlegelberger,B., Schirmacher,P., Kunkel,T.A., Greenberg,R.A., Edelmann,W., and Rudolph,K.L. (**2007**). Exonuclease-1 deletion impairs DNA damage signaling and prolongs lifespan of telomere-dysfunctional mice. **Cell** *130*, 863-877.
(* *these authors contributed equally to this work*)

Erklärung zur Dissertation

Hierdurch erkläre ich, dass die Dissertation

Role of EXO1 and 53BP1 in DNA damage signalling.

selbstständig verfasst und alle benutzten Hilfsmittel sowie evtl. zur Hilfeleistung herangezogene Institutionen vollständig angegeben wurden.

Die Dissertation wurde nicht schon als Diplom-oder ähnliche Prüfungsarbeit verwendet.

Hannover, den

_____ Sept 24' 2008
(Unterschrift)

Name: Kodandaramireddy Nalapa reddy